
LeanVec: Searching vectors faster by making them fit

Mariano Tepper*
Ishwar Singh Bhati*
Cecilia Aguerrebere
Mark Hildebrand
Ted Willke
Intel Labs

mariano.tepper@intel.com
ishwar.s.bhati@intel.com
cecilia.aguerrebere@intel.com
mark.hildebrand@intel.com
ted.willke@intel.com

Abstract

Modern deep learning models have the ability to generate high-dimensional vectors whose similarity reflects semantic resemblance. Thus, similarity search, i.e., the operation of retrieving those vectors in a large collection that are similar to a given query, has become a critical component of a wide range of applications that demand highly accurate and timely answers. In this setting, the high vector dimensionality puts similarity search systems under compute and memory pressure, leading to subpar performance. Additionally, cross-modal retrieval tasks have become increasingly common, e.g., where a user inputs a text query to find the most relevant images for that query. However, these queries often have different distributions than the database embeddings, making it challenging to achieve high accuracy. In this work, we present LeanVec, a framework that combines linear dimensionality reduction with vector quantization to accelerate similarity search on high-dimensional vectors while maintaining accuracy. We present LeanVec variants for in-distribution (ID) and out-of-distribution (OOD) queries. LeanVec-ID yields accuracies on par with those from recently introduced deep learning alternatives whose computational overhead precludes their usage in practice. LeanVec-OOD uses two novel techniques for dimensionality reduction that consider the query and database distributions to simultaneously boost the accuracy and the performance of the framework even further (even presenting competitive results when the query and database distributions match). All in all, our extensive and varied experimental results show that LeanVec produces state-of-the-art results, with up to 3.7x improvement in search throughput and up to 4.9x faster index build time over the state of the art.

1 INTRODUCTION

High-dimensional embedding vectors, stemming from deep learning models, have become the quintessential data representation for unstructured data, e.g., for images, audio, video, text, genomics, and computer code (e.g., [Devlin et al., 2019](#); [Radford et al., 2021](#); [Shvetsova et al., 2022](#); [Ji et al., 2021](#); [Li et al., 2022](#)). The power of these representations comes from translating semantic affinities into spatial similarities between the corresponding vectors. Thus, searching over massive collections of vectors for the nearest neighbors to a given query vector yields semantically relevant results, enabling a wide range of applications (e.g., [Blattmann et al., 2022](#); [Borgeaud et al., 2022](#); [Karpukhin et al., 2020](#); [Lian et al., 2020](#); [Grbovic et al., 2016](#)).

Among other similarity search approaches, graph-based methods (e.g., [Arya and Mount, 1993](#); [Malkov and Yashunin, 2018](#); [Jayaram Subramanya et al., 2019](#)) stand out with their high accuracy and performance for high-dimensional data [Wang et al. \(2021\)](#). Here, the index consists of a directed graph, where each vertex corresponds to a dataset vector and edges represent neighbor-relationships between vectors so that the graph can be efficiently traversed to find the nearest neighbors in sub-linear time ([Fu et al., 2019](#)).

[Aguerebereg et al. \(2023\)](#) have recently shown that, when properly implemented, graph search is bottlenecked by the memory bandwidth of the system, which is mainly consumed by fetching database vectors from

*Equal contribution

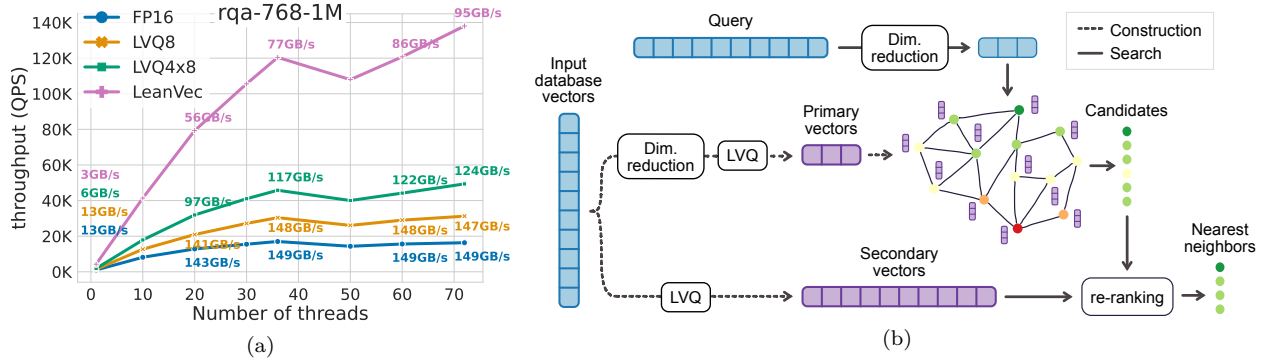


Figure 1: We propose LeanVec, a framework to accelerate similarity search for high-dimensional vectors, including those produced by deep learning models. LeanVec combines a novel linear dimensionality reduction method for in-distribution and out-of-distribution use cases with Locally-adaptive Vector Quantization (LVQ, Aguerrebere et al. (2023)) to achieve state-of-the-art performance and accuracy in graph-based index construction and search. (a) For high dimensional vectors (e.g., $D = 768$), search performance scales with the level of memory compression. Compared to the FP16 encoding, LVQ8 and LVQ4x8 compress the vectors by 2x and ~ 4 x for search, respectively, while LeanVec reduces the vector size by 9.6x (4.8x from dimensionality reduction and 2x from LVQ8). At 72 threads (our system has 36 physical cores and 72 threads), LeanVec provides a 8.5x performance gain over FP16 while consuming much less memory bandwidth (95 vs. 149GB/s). (b) The main search in LeanVec returns nearest neighbor candidates and is executed efficiently using primary vectors, i.e., compressed with dimensionality reduction and vector quantization. The candidates are then re-ranked using secondary vectors, i.e., quantized with LVQ.

memory in a random access pattern (due to the complexity in globally ordering high-dimensional vectors and to the way any graph traversal works, i.e., hoping from one node to the other). Mainstream state-of-the-art vector quantization techniques are either specifically designed for a sequential access pattern (André et al., 2021; Guo et al., 2020), rendering them not suitable for graph search, or incur more expensive similarity calculations by increasing the number of memory accesses (Jégou et al., 2011) (more details in Section 4). To reduce these access times, Aguerrebere et al. (2023) introduce a lightweight method, Locally-adaptive Vector Quantization (LVQ), that greatly accelerates the search and leads to state-of-the-art performance. Although LVQ removes the memory bottleneck in vectors of moderate dimensionality ($D \approx 128$), we observe increased memory bandwidth and computational pressure for higher dimensional (e.g., $D = 512, 768$) deep learning embedding vectors. Higher memory utilization drastically increases the memory latency (Srinivasan et al., 2009) to access each vector and results in suboptimal search performance. Even masterful placement of prefetching instructions in the software cannot hide the increased latency. These difficulties extend to the time-consuming procedure of constructing a graph-based index as construction speed is proportional to search speed. In a world where both academic and industrial deployments of similarity search overwhelmingly use deep learning embedding vectors, it is paramount to address this performance gap.

An additional difficulty with modern applications of similarity search is cross-modal querying, i.e., where a user uses a query from one modality to fetch similar elements from a different modality (Radford et al., 2021; Yu et al., 2022; Li et al., 2023). For instance, in text2image applications, text queries are used to retrieve semantically similar images. Alternatively, sometimes queries and database vectors are produced by different models, e.g., in question-answering applications (Karpukhin et al., 2020). In these cases, queries come from a statistical distribution different from the one underlying the database vectors, which makes applying vector compression techniques learned from the data itself a more challenging problem (Jaiswal et al., 2022).

In this work, we introduce **LeanVec**, a framework that combines linear dimensionality reduction with Locally-adaptive Vector Quantization (LVQ) to accelerate similarity search for high-dimensional vectors, making it suitable for applications with deep learning embedding vectors. LeanVec is inscribed in the standard search-and-rerank paradigm popular in similarity search. We present LeanVec variants for the two main cases: in-distribution (ID) and out-of-distribution (OOD) queries. LeanVec’s compression lowers the

required memory bandwidth and provides a proportional increase in search throughput. On the rqa-768-1M dataset (refer to Table 1 for details), LeanVec compresses vectors by 9.6x (4.8x from the dimensionality reduction and 2x from LVQ) over the baseline of FP16 vectors and provides a 8.5x performance gain while consuming much less memory bandwidth (see Figure 1a). The performance gain increases even further as the dimensionality increases. For instance, in the standard gist-960-1M dataset, LeanVec shows ~12x improvement over the uncompressed FP16 vectors (see Figure 12 in the appendix). We present the following contributions:

- We show that linear dimensionality reduction can be effectively used on-the-fly to increase the performance of graph-based similarity search, with no degradation in quality, and leads to state of the art results for high-dimensional vectors, including those produced by deep learning models.
- We show that LeanVec can be used to build high-quality graph indices in a fraction of the time required for the original vectors, yielding up to a 8.6x runtime improvement.
- For the ID case, LeanVec-ID improves upon previous work using principal component analysis (PCA) (Jegou et al., 2010; Gong et al., 2012; Babenko and Lempitsky, 2014b; Wei et al., 2014) by combining it with LVQ, bringing search speedups of up to 3.6x over the state of the art. LeanVec-ID does not make any assumptions about the statistical distribution of the query vectors.
- For the OOD case, we present a new linear dimensionality reduction technique, LeanVec-OOD, that finds the optimal projection subspaces for the dataset and a representative query set to reduce the errors in the similarity computations. We present two lightweight and fast optimization algorithms for LeanVec-OOD. We present a detailed convergence analysis for one of these variants (based on a non-convex Frank-Wolfe algorithm). We show that LeanVec-OOD performs as good as LeanVec-ID in the ID case and is vastly superior in the OOD case.
- For reproducibility, we will contribute the LeanVec implementation to Scalable Vector Search, an open source library for high-performance similarity search.¹ We also introduce and will open-source two new datasets with different types of OOD characteristics.²

The remainder of this work is organized as follows. We introduce LeanVec in Section 2, covering the overall framework and the novel techniques for OOD dimensionality reduction. We then present in Section 3 extensive experimental results comparing LeanVec to its alternatives and showing its superiority across all relevant metrics. In Section 4 we review the existing literature and its relation to our work. We provide a few concluding remarks in Section 5.

2 LeanVec: a framework to accelerate similarity search for high-dimensional vectors

Notation. We denote vectors/matrices by lowercase/uppercase bold letters, e.g., $\mathbf{v} \in \mathbb{R}^n$ and $\mathbf{A} \in \mathbb{R}^{m \times n}$.

We start from a set of database vectors $\mathcal{X} = \{\mathbf{x}_i \in \mathbb{R}^D\}_{i=1}^n$ to be indexed and searched. We use maximum inner product as the similarity search metric, where one seeks to retrieve for a query \mathbf{q} the k database vectors with the highest inner product with the query, i.e., a set \mathcal{N} such that $\mathcal{N} \subseteq \mathcal{X}$, $|\mathcal{N}| = k$, and $(\forall \mathbf{x}_k \in \mathcal{N}, \forall \mathbf{x}_i \in \mathcal{X} \setminus \mathcal{N}) \langle \mathbf{q}, \mathbf{x}_k \rangle \geq \langle \mathbf{q}, \mathbf{x}_i \rangle$. Although maximum inner product is the most popular choice for deep learning vectors, this choice comes without loss of generality as the common cosine similarity and Euclidean distance we can be trivially mapped to this scenario by normalizing the vectors.

LeanVec accelerates similarity search for deep learning embedding vectors by using the approximation

$$\langle \mathbf{q}, \mathbf{x} \rangle \approx \langle \mathbf{A}\mathbf{q}, \text{quant}(\mathbf{B}\mathbf{x}) \rangle, \quad (1)$$

where $\mathbf{A}, \mathbf{B} \in \mathbb{R}^{d \times D}$ are orthonormal projection matrices, $d < D$, and $\text{quant}(\mathbf{v})$ is a method to quantize each dimension in \mathbf{v} . The projection matrices reduce the number of entries of the database vectors and the quantization reduces the number of bits per entry. The reduced memory footprint decreases the time it takes to fetch each vector from memory. Furthermore, the lower dimensionality alleviates the algorithm’s computational effort (i.e., requiring fewer fused multiply-add operations). This approximation enables efficient

¹<https://github.com/IntelLabs/ScalableVectorSearch>

²<https://github.com/IntelLabs/VectorSearchDatasets>

inner product calculations with individual database vectors (no batch-processing required), which makes it ideal for the random memory-access pattern encountered in graph search.

For the quantization step, we use Locally-adaptive Vector Quantization (LVQ), recently introduced by [Aguerreberre et al. \(2023\)](#), as it is specifically designed to perform encoding/decoding with great efficiency, while incurring negligible search accuracy penalties.

The LeanVec framework is schematically depicted in Figure 1b and its constituents are described next. The computation of the projection matrices will be presented in sections 2.1 to 2.4. In the following, we refer to the set $\{\text{quant}(\mathbf{B}\mathbf{x}_i) \mid \mathbf{x}_i \in \mathcal{X}\}$ as *primary vectors* and to the set $\{\text{quant}(\mathbf{x}_i) \mid \mathbf{x}_i \in \mathcal{X}\}$ as *secondary vectors*.

Search. Here, the primary vectors are used for traversing the graph. We compensate for the errors in the inner-product approximation by retrieving a number of candidates greater than k . Then, we use the set of *secondary vectors*, i.e., $\{\text{quant}(\mathbf{x}_i) \mid \mathbf{x}_i \in \mathcal{X}\}$, to re-compute the inner products for those candidates and to return the top- k . The dimensionality reduction for the query, i.e., the multiplication $\mathbf{A}\mathbf{q}$, is done only once per search incurring a negligible overhead in the overall runtime.

Graph construction. Only the primary vectors are used for graph construction. The secondary vectors are not used at this stage. [Aguerreberre et al. \(2023\)](#) had already analyzed the robustness of the graph construction to quantization with LVQ. Notably, our experimental results show that the robustness extends to a dimensionality reduction as well. It is important to note that searches are an essential part of the graph construction process ([Malkov and Yashunin, 2018](#); [Fu et al., 2019](#)). As such, our achieved search acceleration directly translates into graph construction acceleration, as shown in our experimental results. See Appendix A for a discussion on graph construction and its acceleration.

LeanVec does not use dimensionality reduction to decrease the memory footprint of the similarity search index, but to accelerate its performance. LeanVec, in its current form, effectively increases the total footprint by keeping both primary and secondary vectors in memory. Without loss of generality and in pursuit of a reduced footprint, we could only store to $D - d$ dimensions for the secondary vectors (see the discussion in Section 2.1) which would remove the current overhead. Alternatively, other encodings (e.g., [Douze et al., 2018](#)) can be used for the secondary vectors.

2.1 Dimensionality reduction for in-distribution similarity search

Let us begin with a few standard definitions. The Stiefel manifold is the set of row-orthonormal matrices, formally defined as $\text{St}(D, d) = \{\mathbf{U} \in \mathbb{R}^{d \times D} \mid \mathbf{U}\mathbf{U}^\top = \mathbf{I}\}$. Let $\|\bullet\|_{\text{op}}$ denote the standard spectral norm, defined as $\|\mathbf{A}\|_{\text{op}} = \sup \{\|\mathbf{A}\mathbf{v}\|_2 / \|\mathbf{v}\|_2 \mid \mathbf{v} \in \mathbb{R}^D, \mathbf{v} \neq \mathbf{0}\}$. The convex hull \mathcal{C} of all row-orthonormal matrices in $\text{St}(D, d)$ is the unit-norm ball of the spectral norm, i.e.,

$$\mathcal{C} = \{\mathbf{A} \mid \|\mathbf{A}\|_{\text{op}} \leq 1\}. \quad (2)$$

In the in-distribution (ID) case, we compute the projection matrices from the set of database vectors $\mathcal{X} = \{\mathbf{x}_i \in \mathbb{R}^D\}_{i=1}^n$. Let $d < D$. We use a matrix $\mathbf{M} \in \mathbb{R}^{d \times D}$ to obtain the low-dimensional representation

$$\mathbf{x}_i = \mathbf{M}^\top \mathbf{M}\mathbf{x}_i + \mathbf{e}_i, \quad (3)$$

where $\mathbf{e}_i = (\mathbf{I} - \mathbf{M}^\top \mathbf{M})\mathbf{x}_i$ is the representation error. A desirable characteristic for \mathbf{M} would be to define a d -dimensional orthogonal subspace of \mathbb{R}^D , i.e., $\mathbf{M}\mathbf{M}^\top = \mathbf{I}$. Notice that \mathbf{e}_i can be represented losslessly using $D - d$ dimensions. Commonly, one would seek to find the matrix \mathbf{M} that minimizes the errors \mathbf{e}_i by solving

$$\min_{\mathbf{M} \in \text{St}(D, d)} \left\| \mathbf{X} - \mathbf{M}^\top \mathbf{M}\mathbf{X} \right\|_F^2, \quad (4)$$

where the matrix $\mathbf{X} \in \mathbb{R}^{D \times n}$ is obtained by horizontally stacking the database vectors. This is the traditional Principal Component Analysis (PCA) problem, whose solution is given by keeping the d left singular vectors of \mathbf{X} that correspond to the singular values with larger magnitudes.

With our representation, we approximate $\langle \mathbf{q}, \mathbf{x}_i \rangle \approx \langle \mathbf{q}, \mathbf{M}^\top \mathbf{M}\mathbf{x}_i \rangle = \langle \mathbf{M}\mathbf{q}, \mathbf{M}\mathbf{x}_i \rangle$ and thus $\mathbf{A} = \mathbf{B} = \mathbf{M}$.

2.2 Query-aware dimensionality reduction for out-of-distribution similarity search

From the ID approximation in Equation (3), we get

$$\langle \mathbf{q}, \mathbf{x}_i \rangle - \langle \mathbf{M}\mathbf{q}, \mathbf{M}\mathbf{x}_i \rangle = \langle \mathbf{q}, \mathbf{e}_i \rangle. \quad (5)$$

The smaller the magnitude of $\langle \mathbf{q}, \mathbf{e}_i \rangle$ is, the more accurate the approximation becomes. Observe, however, that Problem (4) can only produce guarantees about $\langle \mathbf{q}, \mathbf{e}_i \rangle$ when the queries and the database vectors are identically distributed. To address this problem, given database vectors $\mathcal{X} = \{\mathbf{x}_i \in \mathbb{R}^D\}_{i=1}^n$ and query vectors $\mathcal{Q} = \{\mathbf{q}_j \in \mathbb{R}^D\}_{j=1}^m$, we propose to minimize the magnitude of $\langle \mathbf{q}_j, \mathbf{e}_i \rangle$ directly.

Thus, given a representative set of query vectors $\mathcal{Q} = \{\mathbf{q}_j \in \mathbb{R}^D\}_{j=1}^m$, we propose the alternative model

$$\mathbf{x}_i = \mathbf{A}^\top \mathbf{B}\mathbf{x}_i + \boldsymbol{\varepsilon}_i, \quad (6)$$

where $\boldsymbol{\varepsilon}_i = (\mathbf{I} - \mathbf{A}^\top \mathbf{B})\mathbf{x}_i$ is the new representation error. We can now minimize $\langle \mathbf{q}_j, \boldsymbol{\varepsilon}_i \rangle^2$ for all i, j , yielding the main optimization problem of this work,

$$\min_{\mathbf{A}, \mathbf{B} \in \text{St}(D, d)} \left\| \mathbf{Q}^\top \mathbf{A}^\top \mathbf{B}\mathbf{X} - \mathbf{Q}^\top \mathbf{X} \right\|_F^2. \quad (7)$$

where $\mathbf{X} \in \mathbb{R}^{D \times n}$ and $\mathbf{Q} \in \mathbb{R}^{D \times m}$ are obtained by horizontally stacking the database and query vectors, respectively. We refer to this dimensionality reduction model as **LeanVec-OOD**. We use LeanVec-OOD for similarity search with the approximation $\langle \mathbf{q}, \mathbf{x}_i \rangle \approx \langle \mathbf{A}\mathbf{q}, \mathbf{B}\mathbf{x}_i \rangle$, where the lower dimensionality alleviates the algorithm’s computational burden (i.e., requiring fewer fused multiply-add operations) while simultaneously reducing memory bandwidth pressure and footprint.

LeanVec-OOD allows suitable matrices for dimensionality reduction to be found and is specifically designed for the case where \mathcal{X} and \mathcal{Q} are not drawn from the same distribution. However, if \mathcal{X} and \mathcal{Q} are drawn from the same distribution, how does LeanVec compare to PCA? The following proposition addresses this question, showing that the LeanVec will perform similarly to PCA in the ID case (the proof is in Appendix B).

Proposition 1. *Problem (7) is upper bounded by the singular value decomposition of \mathbf{X} .*

Proposition 1 ensures that one can run LeanVec-OOD safely, without checking if the query and dataset sets are iso-distributed or not. Of course, LeanVec-OOD comes with the additional requirement of having a representative query set for training. Thankfully, this is not a ominous requirement as the standard calibration of the similarity search system (i.e., finding a suitable operating point in the accuracy-speed trade off for a given application) already requires having a suitable query set.

Interestingly, for the searches performed as part of the graph construction process, database vectors are used as queries implying that, even for OOD use cases, the construction algorithm works with ID data. Proposition 1 ensures that graph construction can be executed with LeanVec-OOD.

Efficiency. Developing the squared Frobenius norm, we can equivalently write Problem (7) as

$$\min_{\mathbf{A}, \mathbf{B} \in \mathcal{C}} \text{Tr} \left(\mathbf{A}\mathbf{K}_\mathbf{Q}\mathbf{A}^\top \mathbf{B}\mathbf{K}_\mathbf{X}\mathbf{B}^\top + \mathbf{K}_\mathbf{Q}\mathbf{K}_\mathbf{X} - 2\mathbf{K}_\mathbf{Q}\mathbf{A}^\top \mathbf{B}\mathbf{K}_\mathbf{X} \right), \quad \text{where } \mathbf{K}_\mathbf{Q} = \mathbf{Q}\mathbf{Q}^\top, \mathbf{K}_\mathbf{X} = \mathbf{X}\mathbf{X}^\top \quad (8)$$

Before solving this problem, we can precompute the $D \times D$ matrices $\mathbf{K}_\mathbf{Q}$ and $\mathbf{K}_\mathbf{X}$. This removes the optimization’s dependency in the number of database and query vectors and enables dealing with large data and query sets with great efficiency. Additionally, relying on the second-order statistics $\mathbf{K}_\mathbf{Q}$ and $\mathbf{K}_\mathbf{X}$ prevents from overfitting the query training set. Moreover, the error between a sample covariance matrix and its expectation converges very quickly (Koltchinskii and Lounici, 2017) with a growing sample size. We can thus safely use uniform subsampling to compute $\mathbf{K}_\mathbf{Q}$ and $\mathbf{K}_\mathbf{X}$, as observed in figures 15 and 16 of the appendix. We need a minimum of D samples (D query and D database vectors) to ensure that these matrices are not artificially rank-deficient. Using $m = 10^4$ queries and $n = 10^5$ database vectors for training amounts to a 13x (20x) query oversampling for $D = 512$ ($D = 768$) over the minimum number of samples D .

Algorithm 1: Frank-Wolfe BCD optimization for Problem (9) with factor $\alpha \in (0, 1)$.

```

1 Let  $\mathbf{A}^{(0)}, \mathbf{B}^{(0)} \in \mathcal{C}$ , e.g.,  $\mathbf{A}^{(0)} \leftarrow \mathbf{0}$  and  $\mathbf{B}^{(0)} \leftarrow \mathbf{0}$ ;
2 for  $t = 0, \dots, T$  do
3    $\gamma \leftarrow 1/(t+1)^\alpha$ ;
4    $\mathbf{S}_A^{(t)} \leftarrow \operatorname{argmax}_{\mathbf{S} \in \mathcal{C}} \langle \mathbf{S}, -\frac{\partial}{\partial \mathbf{A}} f(\mathbf{A}^{(t)}, \mathbf{B}^{(t)}) \rangle$ ; ▷ Eq. (13)
5    $\mathbf{A}^{(t+1)} \leftarrow (1-\gamma)\mathbf{A}^{(t)} + \gamma\mathbf{S}_A^{(t)}$ ;
6    $\mathbf{S}_B^{(t)} \leftarrow \operatorname{argmax}_{\mathbf{S} \in \mathcal{C}} \langle \mathbf{S}, -\frac{\partial}{\partial \mathbf{B}} f(\mathbf{A}^{(t+1)}, \mathbf{B}^{(t)}) \rangle$ ; ▷ Eq. (13)
7    $\mathbf{B}^{(t+1)} \leftarrow (1-\gamma)\mathbf{B}^{(t)} + \gamma\mathbf{S}_B^{(t)}$ ;

```

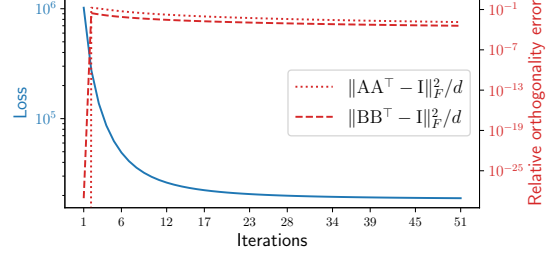


Figure 2: Algorithm 1 converges in 51 iterations for open-images-512-1M with $D = 512$ and $d = 128$. The total runtime is 4 seconds, respectively. Relaxing the orthogonality constraint incurs a relatively small error of 10^{-3} .

2.3 Optimizing the LeanVec-OOD loss with a Frank-Wolfe algorithm

Optimizing Problem (7) is not trivial as it is a constrained optimization problem with a non-convex loss function. Additionally, its constraints are non-convex as the Stiefel manifold is a non-convex set.³ Here, in order to make the optimization of Problem (7) more amenable, we define the relaxed problem

$$\min_{\mathbf{A}, \mathbf{B} \in \mathcal{C}} f(\mathbf{A}, \mathbf{B}), \quad (9)$$

$$\text{where } f(\mathbf{A}, \mathbf{B}) = \left\| \mathbf{Q}^\top \mathbf{A}^\top \mathbf{B} \mathbf{X} - \mathbf{Q}^\top \mathbf{X} \right\|_F^2. \quad (10)$$

Here, we replace the non-convex constraints involving the Stiefel manifold by convex constraints involving its convex hull, Equation (2). Now, Problem (9) is convex and has a smooth loss function on \mathbf{A} for a fixed \mathbf{B} and vice versa. Not only that, but, as we will see next, these convex problems can be solved efficiently. We can thus recur to a block coordinate descent (BCD) method, iteratively fixing one of the variables and updating the other one.

For these subproblems, we use the Frank-Wolfe algorithm (a.k.a. conditional gradient), a classical optimizer for solving a problem with a convex and continuously differentiable loss function f where the variable belongs to a convex set \mathcal{D} (Frank et al., 1956). Given an initial solution $\mathbf{y}^{(0)} \in \mathcal{D}$, the optimization procedure is given by the following iterations for $t = 0, \dots, T$,

$$\mathbf{s} \leftarrow \operatorname{argmax}_{\mathbf{s} \in \mathcal{D}} \langle \mathbf{s}, -\nabla f(\mathbf{y}^{(t)}) \rangle \quad (11)$$

$$\mathbf{y}^{(t+1)} \leftarrow (1-\gamma)\mathbf{y}^{(t)} + \gamma\mathbf{s}. \quad (12)$$

Equation (11) computes the direction in \mathcal{D} that yields the steepest descent, i.e., the one more aligned with $-\nabla f(\mathbf{y}^{(t)})$. The update in Equation (12) guarantees that the iterates remain in \mathcal{D} by using a convex combination of elements in \mathcal{D} .

The function f in Equation (10) has continuous partial derivatives given by $(\mathbf{K}_Q, \mathbf{K}_X)$ defined in Problem (8))

$$\frac{\partial}{\partial \mathbf{A}} f(\mathbf{A}, \mathbf{B}) = 2\mathbf{B}\mathbf{K}_X\mathbf{B}^\top \mathbf{A}\mathbf{K}_Q - 2\mathbf{B}\mathbf{K}_X\mathbf{K}_Q, \quad \text{and} \quad \frac{\partial}{\partial \mathbf{B}} f(\mathbf{A}, \mathbf{B}) = 2\mathbf{A}\mathbf{K}_Q\mathbf{A}^\top \mathbf{B}\mathbf{K}_X - 2\mathbf{A}\mathbf{K}_Q\mathbf{K}_X. \quad (13)$$

We now show that Equation (11) has an efficient solution for our particular subproblems. We can write both updates as $\sup_{\|\mathbf{s}\|_{\text{op}} \leq 1} \langle \mathbf{S}, \mathbf{C} \rangle$, where $\langle \cdot, \cdot \rangle$ is the standard matrix inner product and $\mathbf{C} \in \mathbb{R}^{d \times D}$ stands in either for the $d \times D$ gradient matrices $-\frac{\partial}{\partial \mathbf{A}} f(\mathbf{A}, \mathbf{B})$ or $-\frac{\partial}{\partial \mathbf{B}} f(\mathbf{A}, \mathbf{B})$. This linear problem has a solution

³Recently, Ablin et al. (2023) proposed efficient optimization methods on the Stiefel manifold. We leave the study of this option as future work.

Algorithm 2: Eigenvector search optimization for Problem (15).

- 1 Find $\beta \in [0, 1]$ that minimizes the loss in Problem (14) with $\mathbf{P} \leftarrow \text{projection}(\beta)$;
 - 2 **Procedure** $\text{projection}(\beta)$
 - 3 **return** the matrix $\mathbf{P} \in \text{St}(D, d)$ formed by the d eigenvectors of $\mathbf{K}_\beta = \frac{1-\beta}{m}\mathbf{K}_\mathbf{Q} + \frac{\beta}{n}\mathbf{K}_\mathbf{X}$ with the largest eigenvalues, where $\mathbf{K}_\mathbf{Q} = \mathbf{Q}\mathbf{Q}^\top$ and $\mathbf{K}_\mathbf{X} = \mathbf{X}\mathbf{X}^\top$;
-

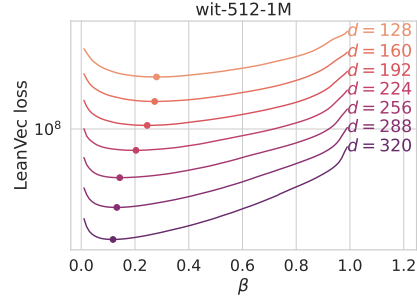


Figure 3: The loss in Problem (14) is a smooth function of β when $\mathbf{P} = \text{eigsearch}(\beta)$ and has a unique minimizer (different for each d). Algorithm 2 finds the minimum (marked with a circle) of this loss. Additional results in Figure 17 of the appendix.

given by $\mathbf{S} = \mathbf{U}\mathbf{V}^\top$, where $\mathbf{U}\mathbf{\Sigma}\mathbf{V}^\top = \mathbf{C}$ is the singular value decomposition of \mathbf{C} (Jaggi, 2013). This update is very efficient for large datasets by working on $d \times D$ matrices.

Equipped with these tools, we can pose the complete optimization procedure in Algorithm 1. There, we update \mathbf{A} (resp. \mathbf{B}) given a fixed \mathbf{B} (resp. \mathbf{A}) by running one Frank-Wolfe update. The factor $\alpha \in (0, 1)$, proposed by Wai et al. (2017) for the step size $\gamma = 1/(t+1)^\alpha$, can be replaced by a line search to speed up the optimization. In our experiments we did not observe a need for such a performance tuning. In practice, we use early termination in Algorithm 1, i.e., we stop the iterations whenever $|f(\mathbf{A}^{(t+1)}, \mathbf{B}^{(t+1)}) - f(\mathbf{A}^{(t)}, \mathbf{B}^{(t)})| / f(\mathbf{A}^{(t)}, \mathbf{B}^{(t)}) \leq 10^{-3}$, yielding a fast runtime, see Figure 2. In Appendix C, we prove the convergence rate of Algorithm 1 to a stationary point of Problem (9).

2.4 Optimizing the LeanVec-OOD loss with eigenvector search

In this section, we assume $\mathbf{A} = \mathbf{B}$. This assumption leads to a new optimization technique for the LeanVec-OOD loss. Given $\mathbf{P} = \mathbf{A} = \mathbf{B}$ and eliminating constant factors, Problem (8) can be rewritten as

$$\min_{\mathbf{P} \in \text{St}(D, d)} \text{Tr} \left(\mathbf{P}\mathbf{K}_\mathbf{Q}\mathbf{P}^\top \mathbf{P}\mathbf{K}_\mathbf{X}\mathbf{P}^\top - 2\mathbf{K}_\mathbf{Q}\mathbf{P}^\top \mathbf{P}\mathbf{K}_\mathbf{X} \right). \quad (14)$$

Here, we can see that it would be desirable to align \mathbf{P} with both the d leading eigenvectors of $\mathbf{K}_\mathbf{Q}$ and with those of $\mathbf{K}_\mathbf{X}$. An intuitive idea would be to set \mathbf{P} using the d leading eigenvectors of $\mathbf{K}_\mathbf{Q} + \mathbf{K}_\mathbf{X}$.

However, the matrices $\mathbf{K}_\mathbf{Q}$ and $\mathbf{K}_\mathbf{X}$ are summations over two different numbers of samples (i.e., n and m are not necessarily equal). This asymmetry would artificially give more weight, for example, to $\mathbf{K}_\mathbf{X}$ if $n \gg m$. We compensate this imbalance by scaling the loss Problem (14) by the constant $\frac{1}{nm}$, obtaining

$$\min_{\mathbf{P} \in \text{St}(D, d)} \text{Tr} \left(\mathbf{P} \left(\frac{1}{m}\mathbf{K}_\mathbf{Q} \right) \mathbf{P}^\top \mathbf{P} \left(\frac{1}{n}\mathbf{K}_\mathbf{X} \right) \mathbf{P}^\top - 2 \left(\frac{1}{m}\mathbf{K}_\mathbf{Q} \right) \mathbf{P}^\top \mathbf{P} \left(\frac{1}{n}\mathbf{K}_\mathbf{X} \right) \right). \quad (15)$$

Now, we could set \mathbf{P} to the d leading eigenvectors of $\frac{1}{m}\mathbf{K}_\mathbf{Q} + \frac{1}{n}\mathbf{K}_\mathbf{X}$. Although an improvement, this equal weighting is not empirically optimal. We thus add a scalar factor $\beta \in \mathbb{R}_+$ and examine the eigenvectors of

$$\mathbf{K}_\beta = \frac{1-\beta}{m}\mathbf{K}_\mathbf{Q} + \frac{\beta}{n}\mathbf{K}_\mathbf{X}. \quad (16)$$

Empirically, we observe in Figure 3 that the loss in Problem (15) is a smooth function of β when $\mathbf{P} \in \mathbb{R}^{d \times D}$ is formed by the d leading eigenvectors of \mathbf{K}_β . Moreover, it has a unique minimizer. Our resulting optimization, summarized in Algorithm 2, uses a derivative-free scalar minimization technique (Brent, 2013) to find the value of β that provides the optimum balance.

In the ID case, we have $\frac{1}{m}\mathbf{K}_\mathbf{Q} = \frac{1}{n}\mathbf{K}_\mathbf{X}$ in expectation. The eigenvectors of \mathbf{K}_β are invariant to the value of β . Hence, in this case, Algorithm 2 offers a seamless fallback, becoming equivalent to Problem (4).

Table 1: Evaluated datasets, where n is the number of database vectors and D their dimensionality. In all cases, we select the target dimensionality d that yields maximum performance at 90% accuracy (10-recall@10). The datasets are originally encoded using 32-bits floating-point values. We use separate learning and test query sets, each with 10K entries. The datasets introduced in this work are marked with a star.

					Dataset	D	n	Similarity	d				
In-distribution	Dataset	D	n	Similarity	d	Out-of-distribution	t2i-200-1M	200	1M	Inner prod.	192		
	gist-960-1M	960	1M	Euclidean	160		t2i-200-10M	200	10M	Inner prod.	192		
	deep-256-1M	256	1M	Euclidean	96		*wit-512-1M	512	1M	Inner prod.	256		
	open-images-512-1M	512	1M	Cosine	160		laion-512-1M	512	1M	Inner prod.	320		
	open-images-512-13M	512	13M	Cosine	160		*rqa-768-1M	768	1M	Inner prod.	160		
					*rqa-768-10M					768	10M	Inner prod.	160

Algorithm 2 is highly efficient and achieves good local minima of the LeanVec-OOD loss but, so far, lacks theoretical guarantees. However, we can use Algorithm 1 to shed light on the quality of the solution \mathbf{P} given by Algorithm 2. If we set $\mathbf{A}^{(0)} \leftarrow \mathbf{P}$ and $\mathbf{B}^{(0)} \leftarrow \mathbf{P}$ in Algorithm 1, Algorithm 1 converges in a handful of iterations, improving the loss by less than 2% as observed in Figure 18 of the appendix (we use line search for the gradient step γ , to ensure that we stay within the same basin). We observe empirically that the theoretical guarantees of Algorithm 1 translate to the solutions of Algorithm 2 and posit that further theoretical analysis may help clarify its empirical performance. Lastly, we point out that both algorithms perform similarly in the end-to-end similarity search evaluation (see Figure 18 of the appendix).

3 Experimental results

We integrated the proposed LeanVec into the state-of-the-art Scalable Vector Search (SVS) library (Aguerreberre et al., 2023) and now present its performance improvements over the state-of-the-art techniques and open-source libraries for graph search and construction. Diverse ablation studies show the impact of the different hyperparameters such as, for example, the target dimensionality d and the quantization level.

Datasets. We evaluate the effectiveness of our method on a wide range of datasets with varied sizes ($n = 1\text{M}$ to $n = 13\text{M}$) and medium to high dimensionalities ($D = 200$ to $D = 960$), containing in-distribution (ID) and out-of-distribution (OOD) queries, see Table 1. For ID and OOD evaluations, we use standard and recently introduced datasets (Zhang et al., 2022; Babenko and Lempitsky, 2021; Schuhmann et al., 2021; Aguerreberre et al., 2024). We also introduce new datasets with different types of OOD characteristics: cross-modality with wit-512-1M and question-answering with rqa-768-1M and 10M. See Appendix E for more details.

Setup. Throughout the experiments, LeanVec uses LVQ8 for the primary vectors and FP16 for the secondary vectors. For each dataset, we use the dimensionality d that yields the highest search performance at 90% accuracy (see Table 1). For LeanVec-OOD, we present the results using Algorithm 1 (Algorithm 2 performs similarly as shown in Figure 13 of the appendix.) To prevent overfitting, we use two separate query sets (see Appendix E): one to learn the LeanVec-OOD projection matrices and to calibrate the runtime search parameters in SVS, and one to generate our results. As standard (Aumüller et al., 2020a), we report the best out of 10 runs for each method. Further experimental details can be found in Appendix D, including a discussion on hyperparameter selection in Appendix D.2.

Search performance. For this study, we use the graph built with uncompressed FP16 vectors to evaluate the search performance gains provided by LeanVec over the state-of-the-art methods in SVS on high-dimensional embedding vectors. Figures 4 and 5 show the search performance on datasets with in-distribution (ID) and out-of-distribution queries, respectively. In the ID datasets, both LeanVec-ID and LeanVec-OOD show similar performance, confirming Proposition 1 in practice. LeanVec-OOD provides up to 10.2x and 3.7x performance gains over FP16 and LVQ, respectively, at a 10-recall@10 of 0.90 on gist-960-1M as it has the highest dimensionality amongst the evaluated datasets (recall is defined in Appendix D.3). LeanVec-OOD shines on the OOD datasets, outperforming LeanVec-ID and LVQ by up to 1.5x and 2.8x, respectively, at a

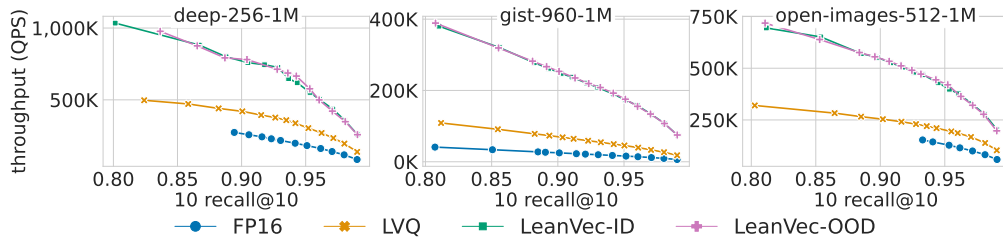


Figure 4: For in-distribution (ID) datasets, LeanVec-ID and LeanVec-OOD show similar performance and vast gains of up to 10.2x and 3.7x over FP16 and LVQ, respectively, for 10-recall@10 of 0.90.

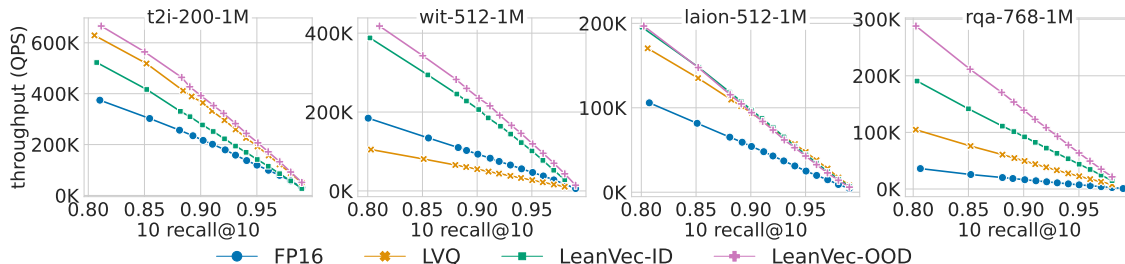


Figure 5: Search performance of LeanVec-OOD shines on out-of-distribution (OOD) datasets, outperforming LeanVec-ID and LVQ by up to 1.5x and 2.8x, respectively, for 10-recall@10 of 0.90.

10-recall@10 of 0.90 on rqa-768-1M. Note that the performance advantage of LeanVec diminishes when the dimensionality of the dataset is small, as in the case of t2i-200-1M. Lastly, LeanVec does not show significant gains in laion-512-1M. In this case, linear dimensionality reduction significantly impacts the accuracy of the search. We plan to address this issue in future work.

Index construction. LeanVec builds graphs up to 8.6x and 4.9x faster than FP16 and LVQ (Figure 6) without degrading their quality, i.e., their search accuracy and speed (see Figure 14 in the appendix). The accuracy preservation is a surprising fact, as the graph, being related to the Delaunay graph, is heavily related to the local topology of the data. Further theoretical studies to understand this phenomenon are required. In LeanVec’s construction timings, we include the time to learn the projection matrices. We point out that the LeanVec-OOD learning (Section 2.2) is implemented in Python, which can be easily optimized.

Comparison with the state of the art. In addition to the state-of-the-art SVS-LVQ (Aguerreberre et al., 2023), we compare LeanVec to three widely adopted methods: HNSWlib (Malkov and Yashunin, 2018), Vamana (Jayaram Subramanya et al., 2019), and FAISS-IVFPQfs (Johnson et al., 2021). See Appendix D for further experimental details and configurations. Here, we use LeanVec-OOD as it achieves equal or better performance than LeanVec-ID in all cases. As shown in Figure 7, the combination of LeanVec with the SVS library achieves a significant performance lead over the other prevalent similarity search methods on high-dimensional datasets. SVS-LeanVec provides 1.1x, 1.9x, 2.8x, and 3.7x performance boost on t2i-200-1M, deep-256-1M, rqa-768-1M, and gist-960-1M, respectively, at a 10-recall@10 of 0.90 over the second-best method, SVS-LVQ, and 2.4x, 3.8x, 7.8x, and 8.5x, respectively, over the third-best method, FAISS-IVFPQfs. Note that the advantage gets higher as the dimensionality increases.

LeanVec scaling on larger datasets. We run LeanVec on three datasets of 13 and 10 million vectors: open-images-512-13M, rqa-768-10M, and t2i-200-10M. As shown in Figure 8, LeanVec continues to show performance gains in larger datasets. LeanVec-OOD achieves 2x and 2.4x performance benefits over LVQ in open-images-512-13M and rqa-768-10M, respectively, at a 10-recall@10 of 0.90. Leaving SVS-LVQ aside, LeanVec-OOD provides much higher benefits when compared to the next best performing methods: 7.9x and 13.7x over HNSWlib in open-images-512-13M and rqa-768-10M, respectively. On t2i-200-10M, the benchmark dataset for the OOD track of the NeurIPS’23 Big-ANN competition (Simhadri et al., 2024), we

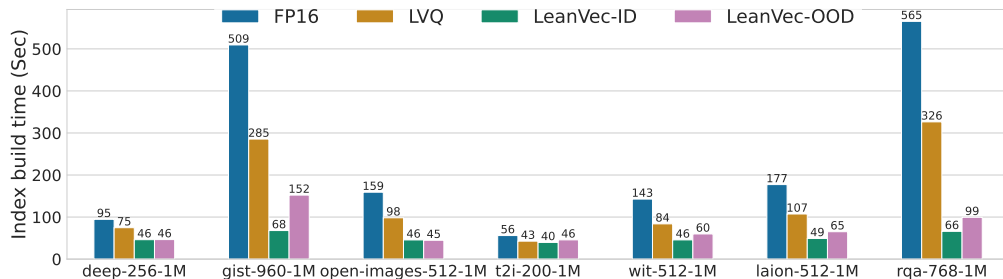


Figure 6: LeanVec accelerates graph construction compared to the state-of-the-art SVS runtimes (by up to 8.6x and 4.9x over FP16 and LVQ, respectively). For OOD datasets, the increase in construction time with LeanVec-OOD over LeanVec-ID brings faster search performance.

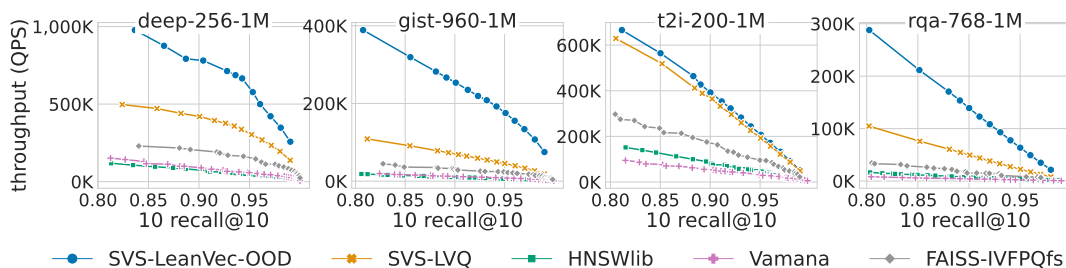


Figure 7: The combination of the state-of-the-art SVS library with LeanVec outperforms other mainstream similarity search methods by a large margin. Compared to FAISS-IVFPQfs, the second-best method outside SVS, SVS-LeanVec provides up to 8.5x performance gain at a 10-recall@10 of 0.90.

consider the track winner RoarANN (Chen et al., 2024). SVS-LeanVec-OOD and SVS-LVQ perform similarly due to the original low-dimensionality ($D = 200$) and outperform RoarANN by 2x at a 10-recall@10 of 0.90.

Ablation study: The target dimensionality. The target dimensionality d required to provide optimal search performance at a given accuracy depends on multiple factors like the system and dataset characteristics. As expected, a lower dimensionality yields higher search throughput at the cost of some accuracy loss. As shown in Figure 9, the performance using values of d that are either too low ($d = 128$) or too high ($d = 320$) for LeanVec-OOD depart from the sweet spot, which is dataset-dependent. With low d , this is due to a loss in accuracy, which we compensate by retrieving more neighbor candidates for the re-ranking step. For high d , the memory and computation costs outweigh the diminishing accuracy improvements. For instance, in gist-960-1M and rqa-768-1M the best performance is reached at $d = 160$, while in wit-512-1M the best performance is attained with $d = 256$.

Ablation study: The level of vector quantization. LeanVec uses dimensionality-reduced primary vectors to fetch nearest neighbor candidates and secondary vectors to re-rank these candidates (see Section 2). Both vectors can be quantized using LVQ. In Figure 10, we study the effect of using different levels of quantization. For the primary vectors, using LVQ outperforms not using compression (FP16) and comes with a lower memory footprint. However, sometimes LVQ4 (using 4 bits per value) is not sufficient, requiring longer search windows to reach the same as LVQ8 (using 8 bits per value). For the secondary vectors, LVQ8 and FP16 provide similar performances except for t2i-200-1M where FP16 does slightly better. If memory footprint is important, we recommend using LVQ8 for the secondary vectors at a minimal cost.

Ablation study: Re-ranking. Figure 11 compares the recall of LeanVec variants with two recent neural network based dimensionality reduction techniques: NN-MDS (Canzar et al., 2021) and CCST (Zhang et al., 2022). To remove confounding factors, we perform exhaustive search for this experiment. NN-MDS and CCST only support the Euclidean distance, thus, for inner-product datasets, we used the transformation by Bachrach et al. (2014) to convert the vectors. Dimensionality is reduced by 4x for each dataset except

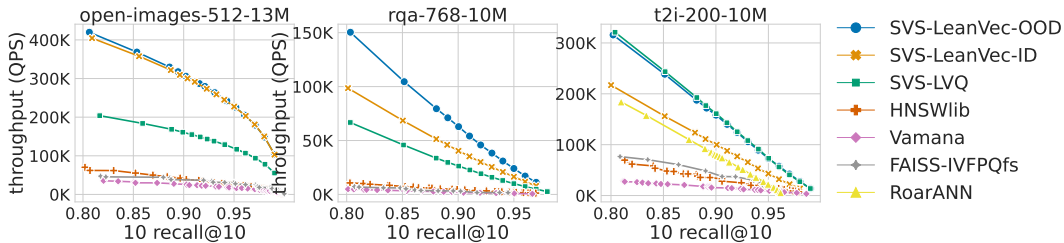


Figure 8: LeanVec exhibits superior performance on large-scale datasets. SVS-LeanVec-OOD achieves performance gains of up to 2.4x over SVS-LVQ and 13.7x over HNSWlib at a 10-recall@10 of 0.90. On t2i-200-10M, compared to RoarANN (Chen et al., 2024), the OOD track winner of the NeurIPS’23 Big-ANN competition (Simhadri et al., 2024), SVS-LeanVec and SVS-LVQ provide 2x performance gain at a 10-recall@10 of 0.90.

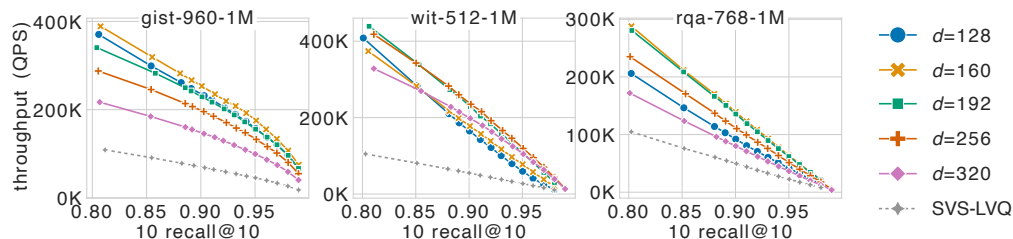


Figure 9: The level of dimensionality reduction at which LeanVec provides the best performance varies for each dataset. However, in all cases, LeanVec brings clear performance improvements over SVS-LVQ, a state-of-the-art solution that does not involve dimensionality reduction. There is a tradeoff between the accuracy and search performance at different target dimensionalities d . In most cases, setting $d = 256$ is a reasonable compromise with 2-3x bandwidth reduction.

t2i-200-1M where we reduce by 2x.⁴ For all three methods, the recall at 10 is unacceptably low (e.g., below 0.90). However, the recall at 50 improves drastically. This observation supports the use of re-ranking, as we can obtain 50 candidates, recompute their distance using secondary vectors to yield a recall at 10 on par with the recall at 50. LeanVec-OOD shows higher recalls than LeanVec-ID on datasets with OOD queries (t2i-200-1M and rqa-768-1M). Note that NN-MDS and CCST use complex neural networks to transform the vectors in low dimensionality, precluding their use for search as the query transformation time is exorbitant.

4 Related Work

The application of linear dimensionality reduction for approximate nearest neighbor search is not new (Deerwester et al., 1990; Ailon and Chazelle, 2009). A few studies (Jegou et al., 2010; Gong et al., 2012; Babenko and Lempitsky, 2014b; Wei et al., 2014) used it for ID queries while the OOD case has been largely ignored.

Hashing (Indyk and Motwani, 1998; Jafari et al., 2021) and learning-to-hash (Wang et al., 2018; Luo et al., 2023) techniques often struggle to simultaneously achieve high accuracy and high speeds.

Product Quantization (PQ) (Jégou et al., 2011) and other related methods (Ge et al., 2013; Babenko and Lempitsky, 2014a; Zhang et al., 2014; André et al., 2015; Matsui et al., 2018; Guo et al., 2020; Wang and Deng, 2020; Johnson et al., 2021; André et al., 2021; Ko et al., 2021) were introduced to handle large datasets in settings with limited memory capacity (e.g., Jayaram Subramanya et al., 2019; Jaiswal et al., 2022). With these techniques, the similarity between (partitions of) the query and each corresponding centroid is precomputed to create a look-up table of partial similarities. The complete similarity computation can then be posed as a set of indexed gather and accumulate operations on this table, which are generally quite slow (Pase and Agelastos, 2019). This is exacerbated with an increased dimensionality D : the lookup table does not fit in L1 cache, which slows down the gather operation even further. Quicker ADC (André et al., 2021)

⁴t2i-200-1M requires $d > 100$ to reach acceptable recalls, but CCST only allows the reduction in factors of 2.

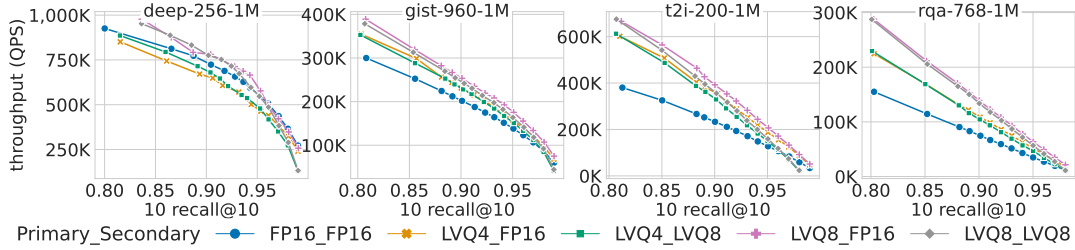


Figure 10: LeanVec-OOD performance sensitivity to different compression schemes used for the primary and secondary vectors. Primary vectors show higher performance when compressed with LVQ8. For the secondary vectors, LVQ8 and FP16 yield similar performance except t2i-200-1M where FP16 does better.

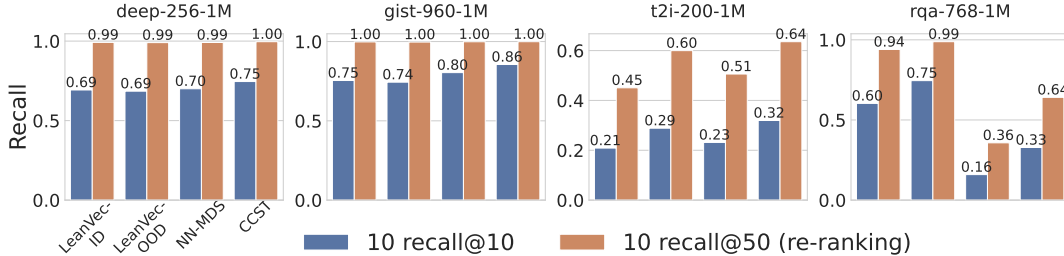


Figure 11: The recall at 10 of all dimensionality reduction techniques suffer (blue bars). However, recall at 50 remains strong. Thus, after selecting 50 candidates and re-ranking them, recall at 10 reaches optimal levels. Like other state-of-the-art techniques, both LeanVec variants show perfect recall on ID datasets, while LeanVec-OOD proves superior in OOD datasets. NN-MDS and CCST employ neural networks for non-linear dimensionality reduction, whose computational complexity precludes their use for search.

offers a clever fix by optimizing these table lookup operations using AVX shuffle and blend instructions to compute the similarity between a query and multiple database elements in parallel. This parallelism can only be achieved if the database elements are stored contiguously in a transposed fashion. This transposition, and Quicker ADC by extension, are ideally suited for inverted indices (Johnson et al., 2021) but are not compatible with the random memory access pattern in graph-based similarity search.

Dimensionality reduction is deeply related to metric learning (Bellet et al., 2013). In the ID case, any metric learned for the main dataset will be equally suitable for similarity search. However, this metric may be unsuitable for similarity search in the OOD case. As an instance of deep metric learning (Kaya and Bilge, 2019), CCST (Zhang et al., 2022) uses transformers to reduce the dimensionality of deep learning embedding vectors. However, the computational complexity of transformers precludes their usage for search and circumscribes their application to index construction, where they lead to significant performance gains. LeanVec outperforms CCST for index construction (Figure 11) and can be equally used for search.

Lastly, He et al. (2021) and Izacard et al. (2020) used PCA in the context of retrieval-augmented language models, showing that their perplexity score is maintained and their overall speed is boosted. However, they treat the similarity search system as a black box and do not address out-of-distribution aspects.

5 CONCLUSIONS

In this work, we presented LeanVec, a framework that combines linear dimensionality reduction with vector quantization to accelerate similarity search on high-dimensional vectors, including those produced by deep learning models. Additionally, LeanVec speeds up the time-consuming construction of the index used to conduct the search. We presented LeanVec variants for in-distribution (ID) and out-of-distribution (OOD) queries, both leading to state-of-the-art results. LeanVec-OOD uses two novel techniques for dimensionality reduction that consider the query and database distributions to simultaneously boost the accuracy and the

performance of the framework even further (even matching the performance of LeanVec-ID in the ID setting). Overall, our extensive and varied experiments show that LeanVec yields state-of-the-art results, with an up to 3.7x improvement in search throughput and up to 4.9x faster index build time over the best alternatives.

As future work, we will investigate why laion-512-1M is resistant to higher levels of linear dimensionality reduction (and whether this behavior extends to other datasets) and propose a solution. We also plan to optimize the LeanVec-OD learning algorithm, implementing it in C++ using [Intel® OneMKL \(2023\)](#).

References

- Ablin, P., Vary, S., Gao, B. and Absil, P.-A. (2023), ‘Infeasible deterministic, stochastic, and variance-reduction algorithms for optimization under orthogonality constraints’, *preprint arXiv:2303.16510*.
- Aguerreberre, C., Bhati, I., Hildebrand, M., Tepper, M. and Willke, T. (2023), ‘Similarity search in the blink of an eye with compressed indices’, *Proceedings of the VLDB Endowment* **16**(11), 3433–3446.
- Aguerreberre, C., Hildebrand, M., Bhati, I., Willke, T. and Tepper, M. (2024), ‘Locally-adaptive quantization for streaming vector search’, *Unpublished manuscript*.
- Ailon, N. and Chazelle, B. (2009), ‘The fast Johnson–Lindenstrauss transform and approximate nearest neighbors’, *SIAM Journal on Computing* **39**(1), 302–322.
- André, F., Kermarrec, A.-M. and Scouarnec, N. L. (2021), ‘Quicker ADC : Unlocking the hidden potential of product quantization with SIMD’, *IEEE Transactions on Pattern Analysis and Machine Intelligence* **43**(5), 1666–1677.
- André, F., Kermarrec, A.-M. and Le Scouarnec, N. (2015), ‘Cache locality is not enough: High-performance nearest neighbor search with product quantization fast scan’, *Proceedings of the VLDB Endowment* **9**(4), 288–299.
- Arya, S. and Mount, D. M. (1993), Approximate nearest neighbor queries in fixed dimensions, in ‘ACM-SIAM Symposium on Discrete algorithms’, Vol. 93, pp. 271–280.
- Aumüller, M., Bernhardsson, E. and Faithfull, A. (2020a), ‘ANN-Benchmarks: A benchmarking tool for approximate nearest neighbor algorithms’, *Information Systems* **87**, 101374.
- Aumüller, M., Bernhardsson, E. and Faithfull, A. (2020b), ‘Benchmarking nearest neighbors’, <http://ann-benchmarks.com/index.html>. GitHub code: <http://github.com/erikbern/ann-benchmarks/>. Accessed: 20 Oct. 2023.
- Babenko, A. and Lempitsky, V. (2014a), Additive quantization for extreme vector compression, in ‘IEEE Conference on Computer Vision and Pattern Recognition’, pp. 931–938.
- Babenko, A. and Lempitsky, V. (2014b), ‘The inverted multi-index’, *IEEE transactions on pattern analysis and machine intelligence* **37**(6), 1247–1260.
- Babenko, A. and Lempitsky, V. (2021), ‘Benchmarks for billion-scale similarity search’, <https://research.yandex.com/blog/benchmarks-for-billion-scale-similarity-search>. Accessed: 15 Feb. 2023.
- Bachrach, Y., Finkelstein, Y., Gilad-Bachrach, R., Katzir, L., Koenigstein, N., Nice, N. and Paquet, U. (2014), Speeding up the Xbox recommender system using a euclidean transformation for inner-product spaces, in ‘ACM Conference on Recommender systems’.
- Bellet, A., Habrard, A. and Sebban, M. (2013), ‘A survey on metric learning for feature vectors and structured data’, *preprint arXiv:1306.6709*.
- Blattmann, A., Rombach, R., Oktay, K., Müller, J. and Ommer, B. (2022), ‘Retrieval-augmented diffusion models’, *Advances in Neural Information Processing Systems* **35**, 15309–15324.

-
- Borgeaud, S., Mensch, A., Hoffmann, J., Cai, T., Rutherford, E., Millican, K., Van Den Driessche, G. B., Lespiau, J.-B., Damoc, B., Clark, A. et al. (2022), Improving language models by retrieving from trillions of tokens, *in* ‘International Conference on Machine Learning’, pp. 2206–2240.
- Brent, R. P. (2013), *Algorithms for minimization without derivatives*, Courier Corporation.
- Canzar, S., Do, V. H., Jelić, S., Laue, S., Matijević, D. and Prusina, T. (2021), ‘Metric multidimensional scaling for large single-cell data sets using neural networks’, *preprint bioRxiv:2021.06.24.449725* .
- Chen, M., Chen, Y., Ma, R., Zhang, K., Cai, Y., Shi, J., Chen, Y. and Zheng, W. (2024), ‘RoarANN: Projected bipartite graph for efficient cross-modal approximate nearest neighbor search’, <https://github.com/matchyc/mysteryann>.
- Deerwester, S., Dumais, S. T., Furnas, G. W., Landauer, T. K. and Harshman, R. (1990), ‘Indexing by latent semantic analysis’, *Journal of the American Society for Information Science* **41**(6), 391–407.
- Devlin, J., Chang, M.-W., Lee, K. and Toutanova, K. (2019), BERT: pre-training of deep bidirectional transformers for language understanding, *in* ‘Conference of the North American Chapter of the Association for Computational Linguistics: Human Language Technologies’, pp. 4171–4186.
- Douze, M., Sablayrolles, A. and Jégou, H. (2018), Link and code: Fast indexing with graphs and compact regression codes, *in* ‘Proceedings of the IEEE conference on computer vision and pattern recognition’, pp. 3646–3654.
- Frank, M., Wolfe, P. et al. (1956), ‘An algorithm for quadratic programming’, *Naval Research Logistics Quarterly* **3**(1-2), 95–110.
- Fu, C., Xiang, C., Wang, C. and Cai, D. (2019), ‘Fast approximate nearest neighbor search with the navigating spreading-out graph’, *Proceedings of the VLDB Endowment* **12**(5), 461–474.
- Ge, T., He, K., Ke, Q. and Sun, J. (2013), ‘Optimized product quantization’, *IEEE transactions on Pattern Analysis and Machine Intelligence* **36**(4), 744–755.
- Gidel, G., Pedregosa, F. and Lacoste-Julien, S. (2018), Frank-Wolfe splitting via augmented lagrangian method, *in* ‘International Conference on Artificial Intelligence and Statistics’, pp. 1456–1465.
- Gong, Y., Lazebnik, S., Gordo, A. and Perronnin, F. (2012), ‘Iterative quantization: A procrustean approach to learning binary codes for large-scale image retrieval’, *IEEE transactions on pattern analysis and machine intelligence* **35**(12), 2916–2929.
- Grbovic, M., Djuric, N., Radosavljevic, V., Silvestri, F., Baeza-Yates, R., Feng, A., Ordentlich, E., Yang, L. and Owens, G. (2016), Scalable semantic matching of queries to ads in sponsored search advertising, *in* ‘International ACM SIGIR conference on Research and Development in Information Retrieval’, pp. 375–384.
- Guo, R., Sun, P., Lindgren, E., Geng, Q., Simcha, D., Chern, F. and Kumar, S. (2020), Accelerating large-scale inference with anisotropic vector quantization, *in* ‘International Conference on Machine Learning’, pp. 3887–3896.
- He, J., Neubig, G. and Berg-Kirkpatrick, T. (2021), ‘Efficient nearest neighbor language models’, *preprint arXiv:2109.04212* .
- Indyk, P. and Motwani, R. (1998), Approximate nearest neighbors: towards removing the curse of dimensionality, *in* ‘ACM Symposium on Theory of Computing’, pp. 604–613.
- Intel® OneMKL (2023), ‘Developer reference for intel® oneAPI Math Kernel Library - C’, <https://www.intel.com/content/www/us/en/docs/onemkl/developer-reference-c/2023-2/overview.html>.
- Izacard, G., Petroni, F., Hosseini, L., De Cao, N., Riedel, S. and Grave, E. (2020), ‘A memory efficient baseline for open domain question answering’, *preprint arXiv:2012.15156* .

-
- Jafari, O., Maurya, P., Nagarkar, P., Islam, K. M. and Crushev, C. (2021), ‘A survey on locality sensitive hashing algorithms and their applications’, *preprint arXiv:2102.08942*.
- Jaggi, M. (2013), Revisiting Frank-Wolfe: Projection-free sparse convex optimization, *in* ‘International Conference on Machine Learning’, pp. 427–435.
- Jaiswal, S., Krishnaswamy, R., Garg, A., Simhadri, H. V. and Agrawal, S. (2022), ‘OOD-DiskANN: Efficient and scalable graph anns for out-of-distribution queries’, *preprint arXiv:2211.12850*.
- Jayaram Subramanya, S., Devvrit, F., Simhadri, H. V., Krishnaswamy, R. and Kadekodi, R. (2019), ‘DiskANN: Fast accurate billion-point nearest neighbor search on a single node’, *Advances in Neural Information Processing Systems* **32**.
- Jegou, H., Douze, M., Schmid, C. and Perez, P. (2010), Aggregating local descriptors into a compact image representation, *in* ‘IEEE Conference on Computer Vision and Pattern Recognition’, IEEE, pp. 3304–3311.
- Ji, Y., Zhou, Z., Liu, H. and Davuluri, R. V. (2021), ‘DNABERT: pre-trained bidirectional encoder representations from transformers model for DNA-language in genome’, *Bioinformatics* **37**(15), 2112–2120.
- Johnson, J., Douze, M. and Jégou, H. (2021), ‘Billion-Scale similarity search with GPUs’, *IEEE Transactions on Big Data* **7**(3), 535–547.
- Jégou, H., Douze, M. and Schmid, C. (2011), ‘Product quantization for nearest neighbor search’, *IEEE Transactions on Pattern Analysis and Machine Intelligence* **33**(1), 117–128.
- Karpukhin, V., Oguz, B., Min, S., Lewis, P., Wu, L., Edunov, S., Chen, D. and Yih, W.-t. (2020), Dense passage retrieval for open-domain question answering, *in* ‘Conference on Empirical Methods in Natural Language Processing’, pp. 6769–6781.
- Kaya, M. and Bilge, H. Ş. (2019), ‘Deep metric learning: A survey’, *Symmetry* **11**(9), 1066.
- Ko, A., Keivanloo, I., Lakshman, V. and Schkufza, E. (2021), ‘Low-precision quantization for efficient nearest neighbor search’, *preprint arXiv:2110.08919*.
- Koltchinskii, V. and Lounici, K. (2017), ‘Concentration inequalities and moment bounds for sample covariance operators’, *Bernoulli* pp. 110–133.
- Kuznetsova, A., Rom, H., Alldrin, N., Uijlings, J., Krasin, I., Pont-Tuset, J., Kamali, S., Popov, S., Mallocci, M., Kolesnikov, A., Duerig, T. and Ferrari, V. (2020), ‘The Open Images Dataset V4: Unified image classification, object detection, and visual relationship detection at scale’, *International Journal of Computer Vision* **128**(7), 1956–1981.
- Lacoste-Julien, S. (2016), ‘Convergence rate of Frank-Wolfe for non-convex objectives’, *preprint arXiv:1607.00345*.
- Li, J., Li, D., Savarese, S. and Hoi, S. (2023), ‘Blip-2: Bootstrapping language-image pre-training with frozen image encoders and large language models’, *preprint arXiv:2301.12597*.
- Li, Y., Choi, D., Chung, J., Kushman, N., Schrittwieser, J., Leblond, R., Eccles, T., Keeling, J., Gimeno, F., Dal Lago, A. et al. (2022), ‘Competition-level code generation with AlphaCode’, *Science* **378**(6624), 1092–1097.
- Lian, D., Wang, H., Liu, Z., Lian, J., Chen, E. and Xie, X. (2020), LightRec: A memory and search-efficient recommender system, *in* ‘The Web Conference’, pp. 695–705.
- Luo, X., Wang, H., Wu, D., Chen, C., Deng, M., Huang, J. and Hua, X.-S. (2023), ‘A survey on deep hashing methods’, *ACM Transactions on Knowledge Discovery from Data* **17**(1), 1–50.
- Malkov, Y. A. and Yashunin, D. A. (2018), ‘Efficient and robust approximate nearest neighbor search using hierarchical navigable small world graphs’, *IEEE Transactions on Pattern Analysis and Machine Intelligence* **42**(4), 824–836.

-
- Matsui, Y., Uchida, Y., Jegou, H. and Satoh, S. (2018), ‘A survey of product quantization’, *ITE Transactions on Media Technology and Applications* **6**(1), 2–10.
- Pase, D. M. and Agelastos, A. M. (2019), ‘Performance of gather/scatter operations’
URL: <https://www.osti.gov/biblio/1761952>
- Peng, L. and Vidal, R. (2023), ‘Block coordinate descent on smooth manifolds’, *preprint arXiv:2305.14744* .
- Qu, Y., Ding, Y., Liu, J., Liu, K., Ren, R., Zhao, W. X., Dong, D., Wu, H. and Wang, H. (2021), Rock-etQA: An optimized training approach to dense passage retrieval for open-domain question answering, *in* ‘Conference of the North American Chapter of the Association for Computational Linguistics: Human Language Technologies’, pp. 5835–5847.
- Radford, A., Kim, J. W., Hallacy, C., Ramesh, A., Goh, G., Agarwal, S., Sastry, G., Askell, A., Mishkin, P., Clark, J. et al. (2021), Learning transferable visual models from natural language supervision, *in* ‘International Conference on Machine Learning’, pp. 8748–8763.
- Raffel, C., Shazeer, N., Roberts, A., Lee, K., Narang, S., Matena, M., Zhou, Y., Li, W. and Liu, P. J. (2020), ‘Exploring the limits of transfer learning with a unified text-to-text transformer’, *The Journal of Machine Learning Research* **21**, 140:1–140:67.
- Reimers, N. and Gurevych, I. (2020), Making monolingual sentence embeddings multilingual using knowledge distillation, *in* ‘Conference on Empirical Methods in Natural Language Processing’.
- Schuhmann, C., Vencu, R., Beaumont, R., Kaczmarczyk, R., Mullis, C., Katta, A., Coombes, T., Jitsev, J. and Komatsuzaki, A. (2021), ‘LAION-400M: open dataset of clip-filtered 400 million image-text pairs’, *Data Centric AI NeurIPS Workshop* .
- Shvetsova, N., Chen, B., Rouditchenko, A., Thomas, S., Kingsbury, B., Feris, R. S., Harwath, D., Glass, J. and Kuehne, H. (2022), Everything at once-multi-modal fusion transformer for video retrieval, *in* ‘IEEE/CVF Conference on Computer Vision and Pattern Recognition’, pp. 20020–20029.
- Simhadri, H. V., Aumüller, M., Baranchuk, D., Douze, M., Liberty, E., Ingber, A., Liu, F. and Williams, G. (2024), ‘NeurIPS 2023 BigANN challenge - practical vector search’, <https://big-ann-benchmarks.com/neurips23.html>.
- Srinivasan, S., Zhao, L., Ganesh, B., Jacob, B., Espig, M. and Iyer, R. (2009), CMP memory modeling: How much does accuracy matter?, *in* ‘Workshop on Modeling, Benchmarking and Simulation’.
- Wai, H.-T., Lafond, J., Scaglione, A. and Moulines, E. (2017), ‘Decentralized Frank–Wolfe algorithm for convex and nonconvex problems’, *IEEE Transactions on Automatic Control* **62**(11), 5522–5537.
- Wang, J., Zhang, T., Song, J., Sebe, N. and Shen, H. T. (2018), ‘A survey on learning to hash’, *IEEE Transactions on Pattern Analysis and Machine Intelligence* **40**(4), 769–790.
- Wang, M., Xu, X., Yue, Q. and Wang, Y. (2021), ‘A comprehensive survey and experimental comparison of graph-based approximate nearest neighbor search’, *Proceedings of the VLDB Endowment* **14**(11), 1964–1978.
- Wang, R. and Deng, D. (2020), ‘DeltaPQ: Lossless product quantization code compression for high dimensional similarity search’, *Proceedings of the VLDB Endowment* **13**(13), 3603–3616.
- Wei, B., Guan, T. and Yu, J. (2014), ‘Projected residual vector quantization for ANN search’, *IEEE Multi-Media* **21**(3), 41–51.
- Yu, J., Wang, Z., Vasudevan, V., Yeung, L., Seyedhosseini, M. and Wu, Y. (2022), ‘CoCa: Contrastive captioners are image-text foundation models’, *preprint arXiv:2205.01917* .
- Zhang, H., Tang, B., Hu, W. and Wang, X. (2022), Connecting compression spaces with transformer for approximate nearest neighbor search, *in* ‘European Conference on Computer Vision’, pp. 515–530.

Zhang, T., Du, C. and Wang, J. (2014), Composite quantization for approximate nearest neighbor search, *in* ‘International Conference on Machine Learning’, pp. 838–846.

A Speeding up graph construction with dimensionality reduction

In the introduction, we discuss the bottlenecks observed when searching with high-dimensional vectors using a graph index. However, these difficulties extend to the construction process of the graph index itself. In every graph index, the construction process can be divided into two main steps: search and pruning.

We start from a directed graph $G = (\mathcal{X}, E)$, where the database vector set \mathcal{X} is used as the node set and the edge set E is initialized depending on the specific graph-construction algorithm (Malkov and Yashunin, 2018; Jayaram Subramanya et al., 2019), where we may even start with $E = \emptyset$. In order to keep the search complexity bounded, each node in the graph has a maximum out-degree R . To build the graph, we iteratively perform the following update routine for each node $\mathbf{x} \in \mathcal{X}$:

Search We first run the search algorithm using the node \mathbf{x} as the query on the current graph G , seeking a set of \mathcal{C} of approximate nearest neighbors with cardinality larger than R .

Pruning We use \mathcal{C} as a set of candidate nodes to form outgoing edges (or arcs) from \mathbf{x} . To increase the navigability of the graph, a pruning algorithm (Arya and Mount, 1993; Malkov and Yashunin, 2018; Jayaram Subramanya et al., 2019) is run on \mathcal{C} , yielding a set $\mathcal{C}' \subseteq \mathcal{C}$ such that $|\mathcal{C}'| < R$. We then replace all the arcs in E starting from \mathbf{x} with the set $\{(\mathbf{x}, \mathbf{x}') \mid \mathbf{x}' \in \mathcal{C}'\}$. It is important to note that all pruning algorithms rely on computing distances between pairs of vectors in \mathbf{C} .

Any slowdowns caused by working with high-dimensional vectors will carry over directly to the graph construction process. The runtime of the search and pruning algorithms are dominated by fetching high-dimensional vectors from memory and computing distances on them. Zhang et al. (2022) observed that graph construction can be accelerated by reducing the vector dimensionality. However, because the dimensionality reduction technique proposed by Zhang et al. (2022) has a time-consuming inference algorithm (based on transformers), it cannot be applied for search: its runtime exceeds the runtime of the search itself). LeanVec applies equally to the search and graph construction processes by alleviating memory pressure while remaining computationally lean.

Scalability. The graph construction technique detailed above is executed (at least once) for each node in the graph (i.e., for each vector in the database). Thus, the technique scales linearly with the graph size both in the number n of nodes and in the number of edges (this quantity is upper bounded by nR). Consequently, the LeanVec acceleration has a linear impact on the graph construction runtime.

B Proof of Proposition 1

Let $\mathbf{A}, \mathbf{B} \in \text{St}(D, d)$.

$$\left\| \mathbf{Q}^\top \mathbf{A}^\top \mathbf{B} \mathbf{X} - \mathbf{Q}^\top \mathbf{X} \right\|_F^2 \leq \|\mathbf{Q}\|_F^2 \cdot \left\| \mathbf{A}^\top \mathbf{B} \mathbf{X} - \mathbf{X} \right\|_F^2 \quad (17)$$

$$\|\mathbf{Q}\|_F^{-2} \cdot \left\| \mathbf{Q}^\top \mathbf{A}^\top \mathbf{B} \mathbf{X} - \mathbf{Q}^\top \mathbf{X} \right\|_F^2 \leq \left\| \mathbf{A}^\top \mathbf{B} \mathbf{X} - \mathbf{X} \right\|_F^2 \quad (18)$$

Thus,

$$\|\mathbf{Q}\|_F^{-2} \cdot \min_{\mathbf{A}, \mathbf{B} \in \text{St}(D, d)} \left\| \mathbf{Q}^\top \mathbf{A}^\top \mathbf{B} \mathbf{X} - \mathbf{Q}^\top \mathbf{X} \right\|_F^2 \leq \min_{\mathbf{A}, \mathbf{B} \in \text{St}(D, d)} \left\| \mathbf{A}^\top \mathbf{B} \mathbf{X} - \mathbf{X} \right\|_F^2 = \min_{\mathbf{A}, \mathbf{B}} \left\| \mathbf{A}^\top \mathbf{B} \mathbf{X} - \mathbf{X} \right\|_F^2, \quad (19)$$

where the last equality is derived from observing that the linear autoencoder,

$$\mathbf{A}^*, \mathbf{B}^* = \underset{\mathbf{A}, \mathbf{B} \in \mathbb{R}^{d \times D}}{\text{argmin}} \left\| \mathbf{A}^\top \mathbf{B} \mathbf{X} - \mathbf{X} \right\|_F^2 \quad (20)$$

has a solution $\mathbf{A}^*, \mathbf{B}^*$ given by truncating the left singular vectors of \mathbf{X} and, in this case, $\mathbf{A}^*, \mathbf{B}^* \in \text{St}(D, d)$. Finally, without loss of generality, we can re-normalize each query \mathbf{q}_j for $j = 1, \dots, m$ such that $\|\mathbf{q}_j\|_2^2 = m^{-1}$, which yields $\|\mathbf{Q}\|_F^2 = 1$ and

$$\min_{\mathbf{A}, \mathbf{B} \in \text{St}(D, d)} \left\| \mathbf{Q}^\top \mathbf{A}^\top \mathbf{B} \mathbf{X} - \mathbf{Q}^\top \mathbf{X} \right\|_F^2 \leq \min_{\mathbf{A}, \mathbf{B}} \left\| \mathbf{A}^\top \mathbf{B} \mathbf{X} - \mathbf{X} \right\|_F^2. \quad (21)$$

C Convergence analysis of the Frank-Wolfe algorithm for LeanVec-OOD

Gidel et al. (2018) has shown that Frank-Wolfe algorithms are convergent for convex problems over the intersection of convex sets. Lacoste-Julien (2016) proved that Frank-Wolfe converges to a stationary point on non-convex objectives. However, to the best of our knowledge, the case with inexact BCD has not been studied in the literature.

We consider the general constrained problem

$$\min_{z \in \mathcal{D}} f(z), \quad (22)$$

where f is a non-convex and continuously differentiable function and \mathcal{D} is a convex set.

We now present two extensions of $\|\nabla f(z^{(t)})\|$ and the Lipschitz assumption, which are standard in unconstrained optimization, suitable for constrained optimization (Lacoste-Julien, 2016).

Definition 1. The Frank-Wolfe gap at $z^{(t)}$ is defined as

$$g^{(t)} = \max_{s \in \mathcal{D}} \langle s - z^{(t)}, -\nabla f(z^{(t)}) \rangle \geq 0. \quad (23)$$

A point $z^{(t)}$ is a stationary point for the Problem (22) if and only if $g_t = 0$.

Definition 2. The curvature constant C_f of a continuously differentiable function f , with respect to the compact domain \mathcal{D} , is defined as

$$C_f = \sup_{\substack{z, s \in \mathcal{D}, \\ y = x + \gamma(s-x)}} \frac{2}{\gamma^2} (f(y) - f(z) - \langle \nabla f(z), y - z \rangle). \quad (24)$$

Lemma 1 (Jaggi (2013, Lemma 7)). If ∇f is L -Lipschitz continuous on \mathcal{D} , i.e., $\|\nabla f(z) - \nabla f(y)\| \leq L\|z - y\|$, then $C_f \leq L(\text{diam}_{\|\cdot\|}(\mathcal{D}))^2$, where $\text{diam}_{\|\cdot\|}$ denotes the $\|\cdot\|$ -diameter.

In our case, $z = \{\mathbf{A}, \mathbf{B}\}$, f is defined in Equation (10), and $\mathcal{D} = \{z \mid \mathbf{A} \in \mathcal{C} \wedge \mathbf{B} \in \mathcal{C}\}$ for \mathcal{C} defined in Equation (2). \mathcal{D} is convex, being the intersection of two convex sets, and f is a non-convex function of z . The partial derivatives in Equation (13) are linear, and thus L -Lipschitz continuous, and $\text{diam}_{\|\cdot\|}(\mathcal{C})$ is bounded. This implies that the curvature for \mathbf{A} (resp. \mathbf{B}), given a fixed \mathbf{B} (resp. \mathbf{A}) is finite.

We are now ready to state our main convergence result.

Theorem 1. Consider Problem (9) and running Algorithm 1 with step size $\gamma^{(t)} = 1/(t+1)^\alpha$ for some $\alpha \in (0, 1)$ and $T \geq 6$ iterations. Then, it holds that

$$\min_{k \in [T/2+1, T]} \left(g_{\mathbf{A}}^{(k)} + g_{\mathbf{B}}^{(k)} \right) \leq \frac{1}{T^{1-\alpha}} \frac{1-\alpha}{1-(2/3)^{1-\alpha}} (h_0 + C). \quad (25)$$

where $h_{T/2+1} = f(\mathbf{A}^{(T/2+1)}, \mathbf{B}^{(T/2+1)}) - \min_{\mathbf{A}, \mathbf{B} \in \mathcal{C}} f(\mathbf{A}, \mathbf{B})$ is the midway global suboptimality and

$$g_{\mathbf{A}}^{(t)} = \left\langle -\frac{\partial}{\partial \mathbf{A}} f(\mathbf{A}^{(t)}, \mathbf{B}^{(t)}), \mathbf{S}_{\mathbf{A}}^{(t)} - \mathbf{A}^{(t)} \right\rangle, \quad (26)$$

$$g_{\mathbf{B}}^{(t)} = \left\langle -\frac{\partial}{\partial \mathbf{B}} f(\mathbf{A}^{(t+1)}, \mathbf{B}^{(t)}), \mathbf{S}_{\mathbf{B}}^{(t)} - \mathbf{B}^{(t)} \right\rangle \quad (27)$$

are the Frank-Wolfe gaps for \mathbf{A} and \mathbf{B} , respectively. It thus takes at most $O(1/\epsilon^{1/(1-\alpha)})$ iterations to find an approximate stationary point with gap smaller than ϵ .

Proof. Following Algorithm 1, we have $\mathbf{A}^{(t+1)} = \mathbf{A}^{(t)} + \gamma \left(\mathbf{S}_{\mathbf{A}}^{(t)} - \mathbf{A}^{(t)} \right)$. Starting from Definition 2, Frank et al. (1956) and Lacoste-Julien (2016) proved that

$$f(\mathbf{A}^{(t+1)}, \mathbf{B}^{(t)}) - f(\mathbf{A}^{(t)}, \mathbf{B}^{(t)}) \leq \gamma \left\langle \frac{\partial}{\partial \mathbf{A}} f(\mathbf{A}^{(t)}, \mathbf{B}^{(t)}), \mathbf{S}_{\mathbf{A}}^{(t)} - \mathbf{A}^{(t)} \right\rangle + \frac{\gamma^2}{2} C_{f_{\mathbf{A}}} \quad (28)$$

$$\leq -\gamma g_{\mathbf{A}}^{(t)} + \frac{\gamma^2}{2} C_{f_{\mathbf{A}}}. \quad (29)$$

By analogy on \mathbf{B} , we have

$$f(\mathbf{A}^{(t+1)}, \mathbf{B}^{(t+1)}) - f(\mathbf{A}^{(t+1)}, \mathbf{B}^{(t)}) \leq -\gamma g_{\mathbf{B}}^{(t)} + \frac{\gamma^2}{2} C_{f_{\mathbf{B}}} \quad (30)$$

Let $C \geq \max\{C_{f_{\mathbf{A}}}, C_{f_{\mathbf{B}}}\}$. Summing equations (29) and (30), we get

$$f(\mathbf{A}^{(t+1)}, \mathbf{B}^{(t+1)}) - f(\mathbf{A}^{(t)}, \mathbf{B}^{(t)}) \leq -\gamma^{(t)} g_{\mathbf{A}}^{(t)} + \frac{\gamma^2}{2} C - \gamma^{(t)} g_{\mathbf{B}}^{(t)} + \frac{\gamma^2}{2} C \quad (31)$$

$$\leq -\gamma^{(t)} \left(g_{\mathbf{A}}^{(t)} + g_{\mathbf{B}}^{(t)} \right) + \left(\gamma^{(t)} \right)^2 C \quad (32)$$

Now, summing over the steps in $t = T/2 + 1, \dots, T$ steps,

$$f(\mathbf{A}^{(T)}, \mathbf{B}^{(T)}) - f(\mathbf{A}^{(T/2+1)}, \mathbf{B}^{(T/2+1)}) = \sum_{k=T/2+1}^T f(\mathbf{A}^{(k+1)}, \mathbf{B}^{(k+1)}) - f(\mathbf{A}^{(k)}, \mathbf{B}^{(k)}) \quad (33)$$

$$\leq \sum_{k=T/2+1}^T -\gamma^{(k)} \left(g_{\mathbf{A}}^{(k)} + g_{\mathbf{B}}^{(k)} \right) + \left(\gamma^{(k)} \right)^2 C \quad (34)$$

$$\leq - \left(\sum_{k=T/2+1}^T \gamma^{(k)} \right) \min_{t' \in [T/2+1, T]} \left(g_{\mathbf{A}}^{(t')} + g_{\mathbf{B}}^{(t')} \right) + C \sum_{k=T/2+1}^T \left(\gamma^{(k)} \right)^2 \quad (35)$$

Wai et al. (2017, Equation (64)) showed that

$$\sum_{k=T/2+1}^T \gamma^{(k)} \geq \frac{T^{1-\alpha}}{1-\alpha} \left(1 - \left(\frac{2}{3} \right)^{1-\alpha} \right). \quad (36)$$

Additionally,

$$\sum_{k=T/2+1}^T \left(\gamma^{(k)} \right)^2 = \sum_{k=T/2+1}^T \frac{1}{(k+1)^2} \leq 1. \quad (37)$$

Let $h_{T/2+1} = f(\mathbf{A}^{(T/2+1)}, \mathbf{B}^{(T/2+1)}) - \min_{\mathbf{A}, \mathbf{B} \in \mathcal{C}} f(\mathbf{A}, \mathbf{B})$. By definition,

$$f(\mathbf{A}^{(T)}, \mathbf{B}^{(T)}) - f(\mathbf{A}^{(T/2+1)}, \mathbf{B}^{(T/2+1)}) \geq -h_{T/2+1}. \quad (38)$$

Finally, plugging equations (36–38) in Equation (35) we get

$$\min_{t' \in [T/2+1, T]} \left(g_{\mathbf{A}}^{(t')} + g_{\mathbf{B}}^{(t')} \right) \leq \frac{1}{T^{1-\alpha}} \frac{1-\alpha}{1 - (2/3)^{1-\alpha}} (h_0 + C). \quad (39)$$

□

Interestingly, our setting is very related to one in the recent work by Peng and Vidal (2023). They study Problem (22) with a BCD algorithm, but concentrate on the exact minimization of the subproblems or in a case where retractions are applied. We leave as future work the extension of Theorem 1 and its proof to the general setting with more than two blocks.

D Experimental setup.

Without loss of generality, we use the Vamana algorithm (Jayaram Subramanya et al., 2019) to build the graph and standard greedy traversal with backtracking (Fu et al., 2019) for search. Unless specified otherwise, we use the following configurations for graph construction: we set $R = 128$, $L = 200$, $\alpha = 1.2$ for L2 distance, and $\alpha = 0.95$ for inner product.

D.1 Baseline approaches

We use the state-of-the-art Scalable Vector Search (SVS) library as our main baseline with the same graph construction hyperparameters as the ones chosen for LeanVec and its LVQ implementation with the LVQ4x8 scheme (Aguerrebere et al., 2023).

Apart from the state-of-the-art SVS-LVQ (Aguerrebere et al., 2023), we compare LeanVec to three widely adopted methods: HNSWlib (Malkov and Yashunin, 2018), Vamana (Jayaram Subramanya et al., 2019), and FAISS-IVFPQfs (Johnson et al., 2021). For HNSWlib, Vamana, and FAISS-IVFPQfs, we use the configuration settings provided in ANN-benchmarks (Aumüller et al., 2020b) and generate Pareto curves of QPS vs. recall. For Vamana, in addition to the ANN-Benchmark settings, we include the results with graphs built using $R = 128$, $L = 200$, and $\alpha = 1.2$ (the same parameters used to construct SVS graphs).

On the evaluated datasets, we observed no performance benefits of the OOD-DiskANN⁵ (Jaiswal et al., 2022) over the baseline Vamana when using disjoint learning and test query sets.

We also considered RoarANN (Chen et al., 2024), the winner of the OOD track of the NeurIPS’23 Big-ANN competition (Simhadri et al., 2024), using the hyperparameters used by its authors for the competition. RoarANN failed with a segfault while building indices for open-images-512-13M and rqa-768-10M.

D.2 Finding the optimal target dimensionality d

In our experiments, we only vary one parameter to tune the performance: the target dimensionality d . The hyperparameters used to build the indices are set once and shared for all datasets (described in the introductory paragraph of Appendix D). The choice of LVQ-8 for the primary vectors and either LVQ-8 or FP16 for the secondary vectors is consistently superior to the other choices (see Figure 10). Thus, we also keep this choice fixed throughout the experiments.

The target dimensionality d that yields the best performance is dataset dependent as the loss we are optimizing depends on the data distribution (see the ablation study in Figure 9). However, for most datasets whose dimensionality is typical of modern deep learning models, there is an optimum that lies somewhere in the range [160, 256]. Notice that the differences between the achieved performance when d is in this range are not striking. Any of these choices would yield significant improvements over the state of the art. Even a poor choice, like $d = 320$ is in many cases, already provides significant performance gains over the state of the art. A user not seeking to do any hyperparameter tuning will be covered by picking $d \in [160, 256]$.

We point out that tuning d is no different than tuning, for example, the number of segments used in a product quantizer, the number of levels using in a residual quantizer, or the number of clusters used in a traditional vector quantizer. With any vector compression method, its optimal behavior will depend on finding the best fit to a specific data distribution. It is important, though, that its behavior degrades gracefully as we move away from the best-fit hyperparameters. Our experiments show that LeanVec does exhibit such a graceful degradation.

For each dataset, we use the dimensionality d that yields the highest search performance at 90% accuracy (see Table 1). To find this d , we use the same graph built from uncompressed vectors and measure the search throughput by increasing d in steps of 32 starting from 64. This involves building projection matrices, projecting the database vectors for each d , and finally running searches to find the best d .

⁵<https://github.com/microsoft/DiskANN/tree/ood-queries>

D.3 Metrics

Search accuracy is measured by k -recall@ k , defined by $|S \cap G_t|/k$, where S are the ids of the k retrieved neighbors and G_t is the ground-truth. Unless otherwise specified, we use $k = 10$ in all experiments and 0.9 as the default accuracy value. Search performance is measured by queries per second (QPS).

D.4 System setup

We conduct our experiments on a 2-socket 3rd generation Intel® Xeon® 8360Y @2.40GHz CPUs with 36 cores (2x hyperthreading enabled) and 256GB DDR4 memory (@2933MT/s) per socket, running Ubuntu 22.04.⁶ We ran all our experiments using 72 threads on a single socket to avoid introducing performance regressions due to remote NUMA memory accesses. Further, as recommended by [Aguerreberre et al. \(2023\)](#), we use the *hugeadm* Linux utility to preallocate a sufficient number of 1GB huge pages.

E Datasets

We evaluate the effectiveness of our method on a wide range of in-distribution (ID) and out-of-distribution (OOD) datasets as shown in Table 1.

Following the experimental setup by [Zhang et al. \(2022\)](#), we use gist-960-1M and deep-256-1M, two standard high-dimensional ID datasets.⁷ We utilize the learn sets provided in these datasets to construct test and validation query sets, with the first 10K entries as test and the next 10k as validation.

We use the ID datasets open-images-512-1M and open-images-512-13M ([Aguerreberre et al., 2024](#)), with 1 million and 13 million database vectors, generated from a subset Google’s Open Images ([Kuznetsova et al., 2020](#)) using the CLIP model ([Radford et al., 2021](#)). Although built for cosine similarity, we use the equivalent operation of minimizing the Euclidean distances since the vectors in this dataset are normalized. We use the provided queries to represent the test set while the validation set is created from the first 10K entries of the provided learn queries.

For OOD evaluations, we use the first one million vectors from two cross-modal text-to-image datasets, namely t2i-200-1M ([Babenko and Lempitsky, 2021](#)) and laion-512-1M ([Schuhmann et al., 2021](#)), where the query and database vectors are text and image embeddings, respectively. We divide the 10^5 queries provided in t2i-200-1M into a test set (first 10^4 entries) and a learning set (next 10^4 entries). In laion-512-1M, we use the text embeddings in the `text_emb_101.npy` file⁸ to build the query set, using the initial 10^4 for the test set and the next 10^4 for the learning set.

E.1 New text-to-image dataset with OOD queries

We introduce wit-512-1M, a new dataset with OOD queries stemming from a text-to-image application. The WIT dataset⁹ is a multimodal multilingual dataset that contains 37 million rich image-text examples extracted from Wikipedia pages. For each example in the first million, we take the image¹⁰ and encode it using the multimodal OpenAI CLIP-ViT-B32 model ([Radford et al., 2021](#)) to generate a database vector. We create the query set using the first $2 \cdot 10^4$ text descriptions in one of the provided test sets¹¹ (concatenating the Reference and Attribution description fields) and generating the corresponding embeddings using CLIP-

⁶Performance varies by use, configuration and other factors. Learn more at www.intel.com/PerformanceIndex. Performance results are based on testing as of dates shown in configurations and may not reflect all publicly available updates. No product or component can be absolutely secure. Your costs and results may vary. Intel technologies may require enabled hardware, software or service activation. ©Intel Corporation. Intel, the Intel logo, and other Intel marks are trademarks of Intel Corporation or its subsidiaries. Other names and brands may be claimed as the property of others.

⁷<https://www.cse.cuhk.edu.hk/systems/hash/gqr/datasets.html>

⁸file name: `text_emb_101.npy` in https://deploy.laion.ai/8f83b608504d46bb81708ec86e912220/embeddings/text_emb/

⁹<https://github.com/google-research-datasets/wit>

¹⁰Images downloaded from https://storage.cloud.google.com/wikimedia-image-caption-public/image_data_train.tar

¹¹Downloaded from https://storage.googleapis.com/gresearch/wit/wit_v1.test.all-00000-of-00005.tsv.gz

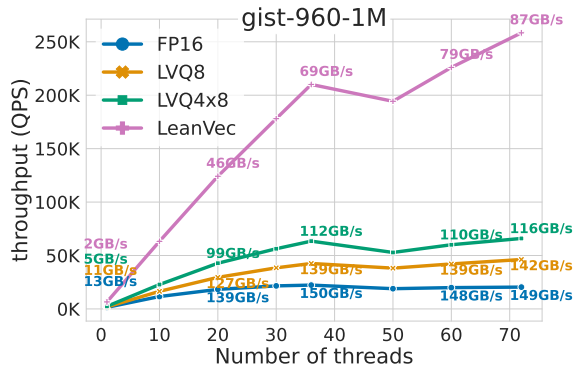


Figure 12: For high dimensional vectors (e.g., $D = 960$), search performance scales with the level of memory compression. Compared to the FP16 encoding, LVQ8 and LVQ4x8 compress the vectors by 2x and ~ 4 x for search, respectively, while LeanVec reduces the vector size by 12x (6x from dimensionality reduction and 2x from LVQ8). At 72 threads (our system has 36 physical cores and 72 threads), LeanVec provides ~ 12 x performance gain over FP16 while consuming much lesser memory bandwidth.

ViT-B32-multilingual-v1 (Reimers and Gurevych, 2020).¹² Finally, for each query, we compute the 100 ground truth nearest neighbors using maximum inner product. We use the first 10^4 queries as a test set and the remaining 10^4 as a learning set.

E.2 New question-answering dataset with ID and OOD queries

We introduce two instances of a new dataset with OOD queries stemming from a question-answering application, rqa-512-1M and rqa-512-10M, respectively with 1M and 10M vectors. Here, we encode text using the RocketQA dense passage retriever model (Qu et al., 2021).¹³ The OOD nature of the queries emerges as dense passage retrievers use different neural networks to encode the questions (i.e, queries) and the answers (i.e., database vectors). We created ID and OOD versions of this dataset, although in the experiments in this paper we use the OOD variant.

We created the vector embeddings using text snippets from AllenAI’s¹⁴ C4 dataset (Raffel et al., 2020) as follows.

- From the data split *en/training*, we generate $10^7 + 2 \cdot 10^4$ snippets (using files *c4-train.00000-of-01024.json.gz* to *c4-train.00032-of-01024*). The first 10^6 and 10^7 snippets are encoded with the answer model to form the database vectors for the 1 and 10 million variants, respectively. The last $2 \cdot 10^4$ snippets are encoded to form the queries of the ID variant, from which we use the first 10^4 as a query learning set and the last 10^4 as a query test set.
- From the data split *en/validation*, we generate $2 \cdot 10^4$ snippets (using file *c4-validation.00000-of-00008.json.gz*). These snippets are encoded with the question model to form the queries of the OOD variant, from which we use the first 10^4 as a query learning set and the last 10^4 as a query test set.

For each query, we compute the 100 ground truth nearest neighbors using maximum inner product as suggested by Karpukhin et al. (2020).

We will soon release the code to generate wit-512-1M, rqa-768-1M, and rqa-768-10M at <https://github.com/IntelLabs/VectorSearchDatasets>.

¹²The use of CLIP-ViT-B32 for images and multi-lingual CLIP-ViT-B32-multilingual-v1 for text follows the protocol suggested in <https://huggingface.co/sentence-transformers/clip-ViT-B-32-multilingual-v1>.

¹³<https://github.com/PaddlePaddle/RocketQA>

¹⁴<https://huggingface.co/datasets/allenai/c4>

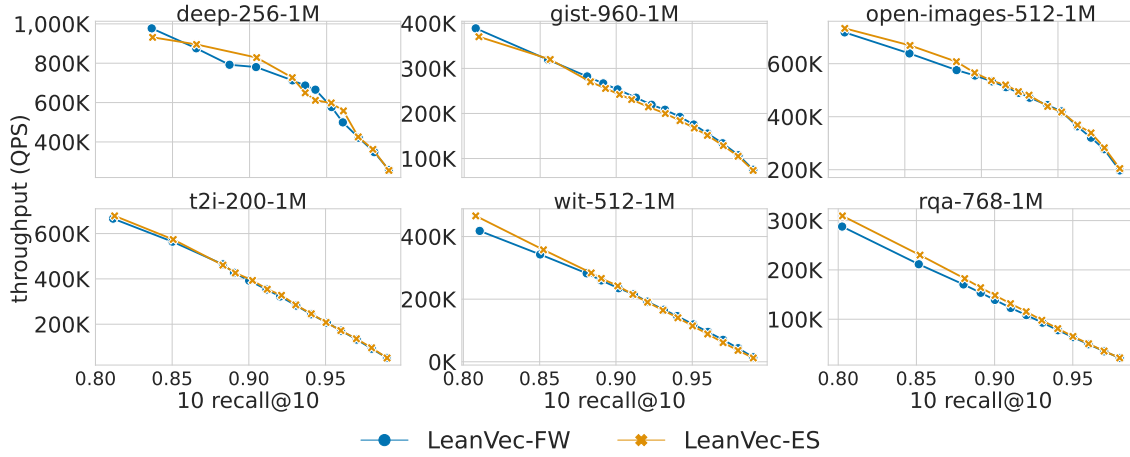


Figure 13: Search throughput and accuracy comparison between the two LeanVec-OOD variants, namely LeanVec-FW (Algorithm 1) and LeanVec-ES (Algorithm 2).

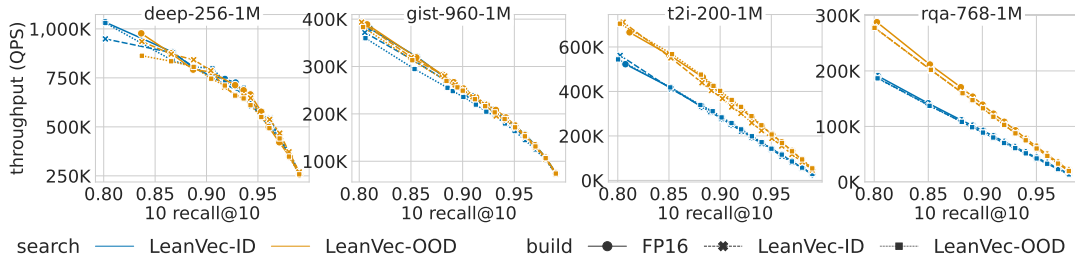


Figure 14: Search throughput and accuracy comparison for different LeanVec combinations. We observe no noticeable differences in the graphs built with and without dimensionality reduction.

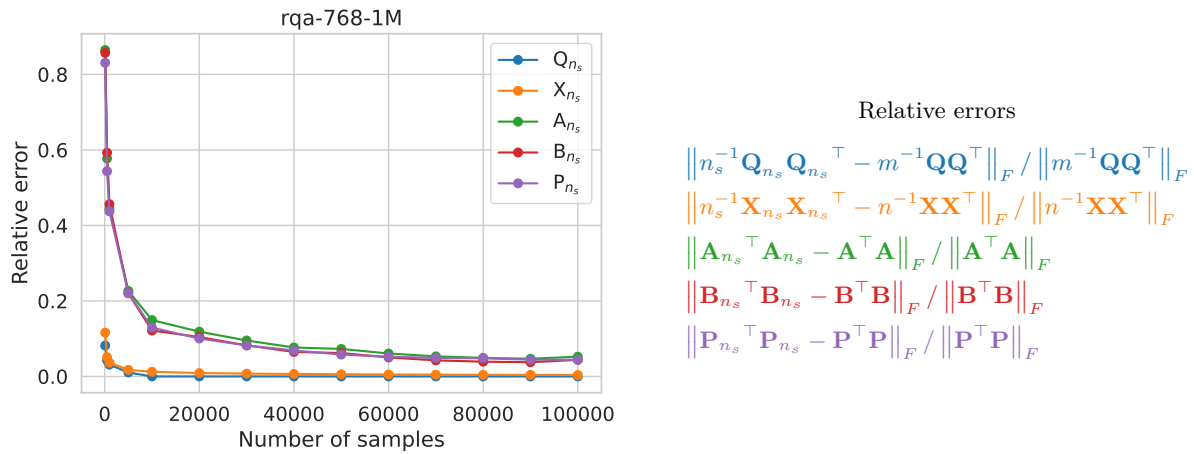


Figure 15: The error between a sample covariance matrix and its expectation converges quickly (Koltchinskii and Lounici, 2017) with a growing sample size (at a \sqrt{n} rate). This quick convergence carries over to the LeanVec-OOD loss being a function of $\mathbf{K}_\mathbf{Q} = \mathbf{Q}\mathbf{Q}^\top$ and $\mathbf{K}_\mathbf{X} = \mathbf{X}\mathbf{X}^\top$. In this experiment, we first optimize the LeanVec-OOD loss, using the full learning sets with $n = 10^6$ database vectors and $m = 10^4$ queries, with Algorithm 1 to obtain \mathbf{A} and \mathbf{B} or with Algorithm 2 to obtain \mathbf{P} . Then, using different numbers n_s of random subsamples to compute $\mathbf{K}_\mathbf{Q}$ and $\mathbf{K}_\mathbf{X}$, we obtain \mathbf{A}_{n_s} , \mathbf{B}_{n_s} , and \mathbf{P}_{n_s} using the corresponding algorithm. We can see that the relative errors (formulas on the right-hand side) drop quickly in the left plot as n_s grows.

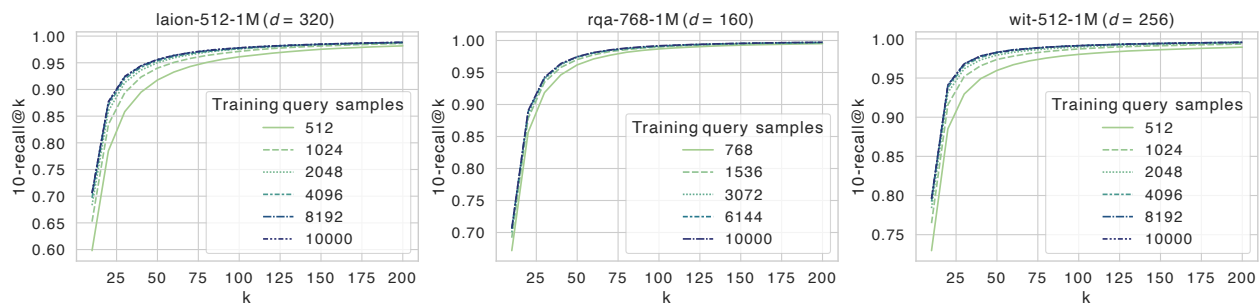


Figure 16: The brute-force search accuracy of LeanVec-ES is robust to subsampling the set of query vectors used for learning/training. Let n_s be this query sample size. Some degradation can be perceived when using $n_s = D$ or $n_s = 2D$ samples but it vanishes when using $n_s = 4D$ samples or more. This result is in agreement with the quick convergence of the matrices \mathbf{K}_Q and \mathbf{K}_X defined in Problem (8) as n_s grows.

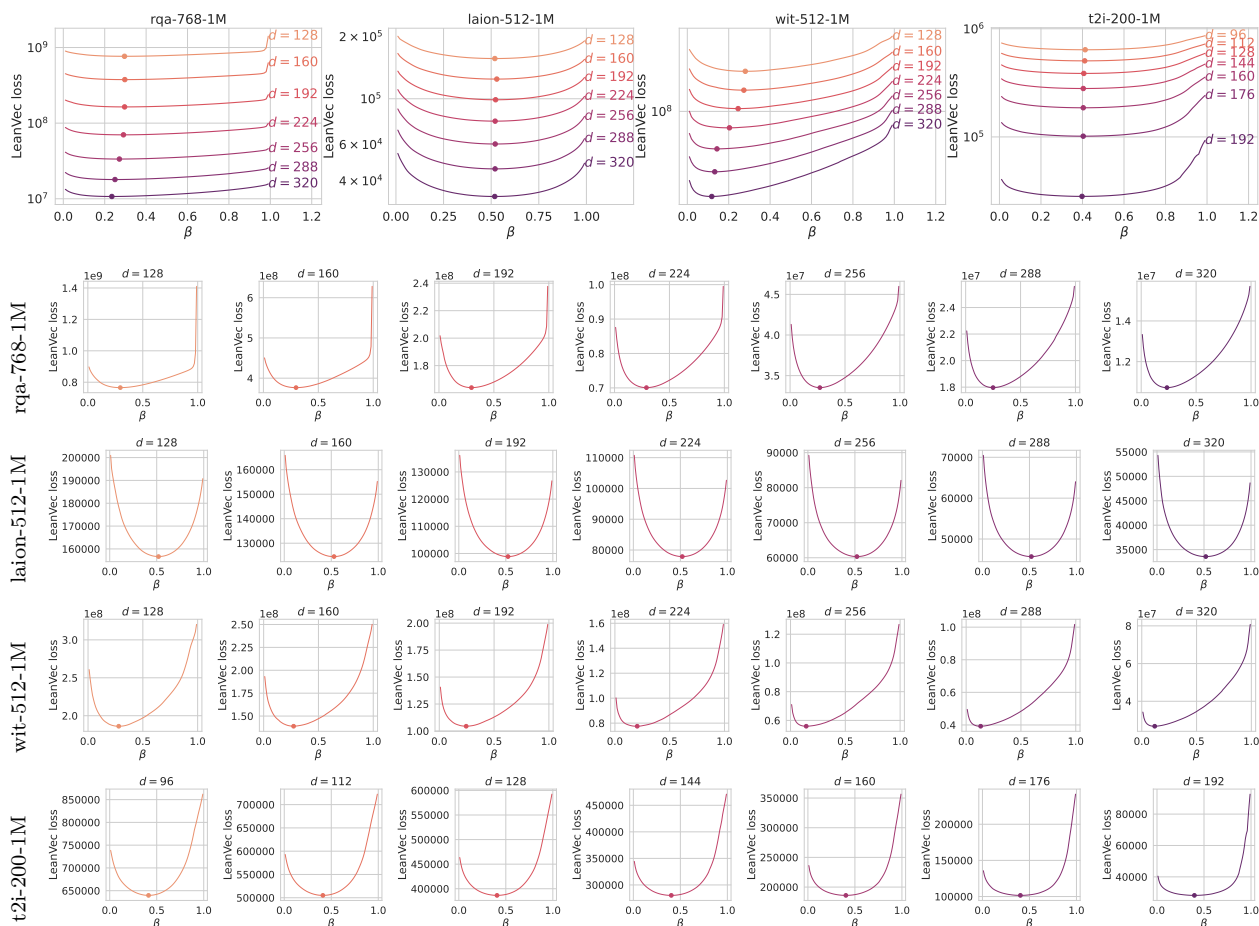


Figure 17: The loss in Problem (14) is a smooth function of β when $\mathbf{P} = \text{eigsearch}(\beta)$ and empirically we observe that it has a unique minimizer (different for each d). Algorithm 2 finds the minimum (marked with a circle) of this loss using a derivative-free scalar minimization. We point out that the solutions with $\beta = 0$ and $\beta = 1$ correspond to the SVD of the query and database vectors, respectively.

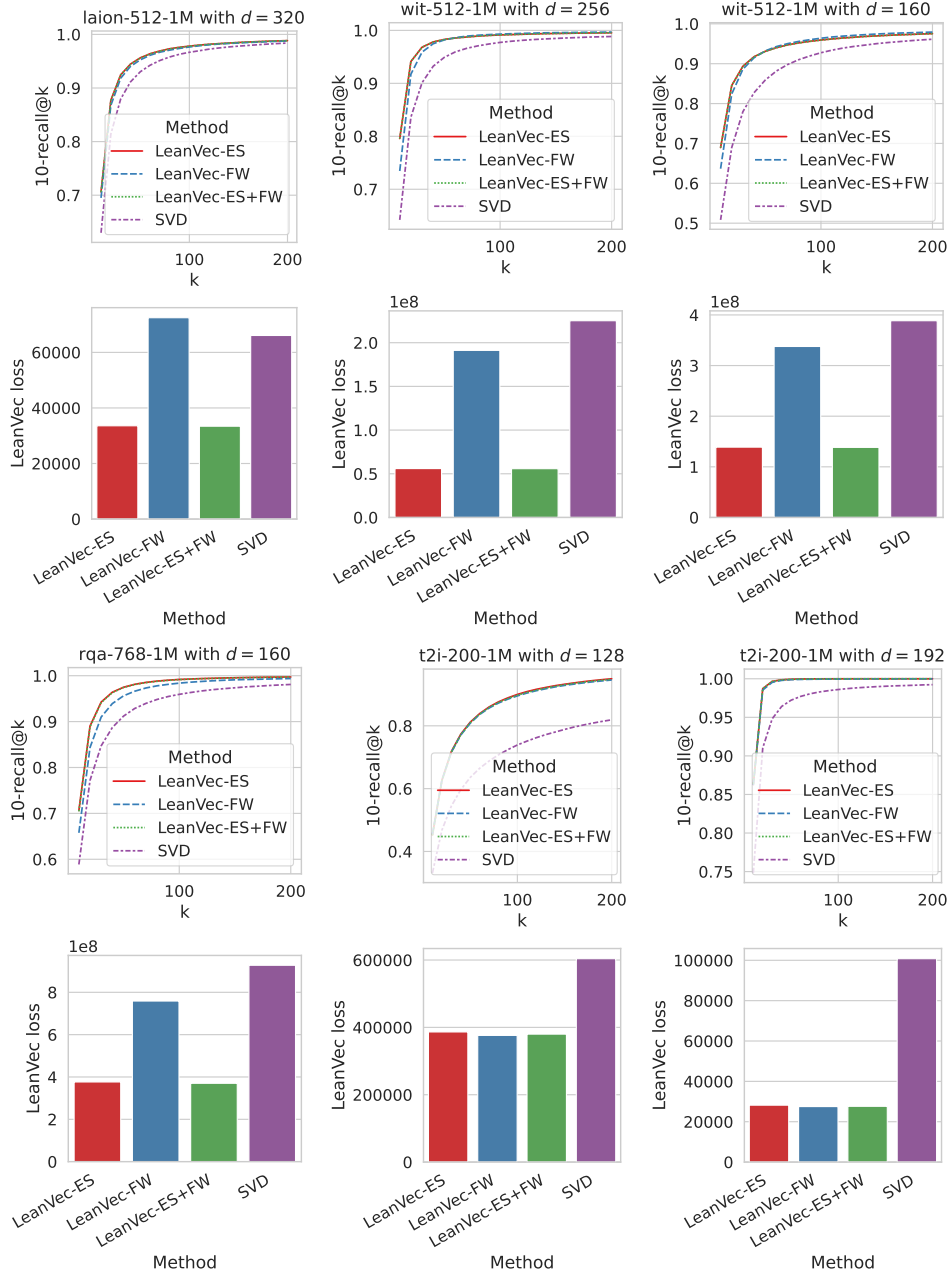


Figure 18: LeanVec-FW, LeanVec-ES, and SVD correspond to Algorithm 1, to Algorithm 2, and to the algorithm in Section 2.1, respectively. LeanVec-ES+FW corresponds to initializing Algorithm 1 with the output of Algorithm 2. Although LeanVec-ES often yields a lower loss value than LeanVec-FW, their brute-force search performance are comparable. The behaviors of LeanVec-ES and LeanVec-ES+FW are almost indistinguishable across the board, bringing assurance about the good empirical performance of LeanVec-ES.